Univerzita Karlova

Přírodovědecká fakulta

Biologie

Buněčná a vývojová biologie - Fyziologie buňky

Bc. Eliška Novotná

Role tyrosinkinázové aktivity mitochondriálního ERBB2/HER2 v rakovině prsu

The Role of Tyrosine Kinase Activity of Mitochondrial ERBB2/HER2 in Breast Cancer

Diplomová práce

Vedoucí závěrečné práce: **Mgr. Jakub Rohlena, Ph.D.**

Praha, 2019

Prohlášení

Prohlašuji, že jsem závěrečnou práci zpracovala samostatně a že jsem uvedla všechny použité informační zdroje a literaturu. Tato práce ani její podstatná část nebyla předložena k získání jiného nebo stejného akademického titulu.

V Praze, 9. 8. 2019

……

Author of the Thesis contributed to the experimental part as following:

The vast majority of experiments was performed by Eliška Novotná. Exceptions are listed below:

Jakub Gemperle assessed migration of studied cells in collagen.
Silvia Novais and Jakub Rohlena performed *in vivo* experiment.
Mirko Milošević partially contributed to cell death and ROS measurements.
Linda Krobová performed western blotting analysis shown in figure 4.3 B.

Acknowledgement

My immense thanks are addressed to Jakub Rohlena for his tireless patience and persistent effort to create a scientist from a tough material that came to the laboratory three years ago. I appreciate I have never heard "No" when I asked for help, even when I could not open the lid of a centrifuge or I asked really stupid questions. I would like to thank to Kateřina Rohlenová being patient when teaching me most of the methods I know and introducing me into this remarkable project. They are behind a substantial portion of my education and I'm very grateful I could spend some time under their supervision.

I would like to further thank namely to Linda Krobová, Silvia Novais and Mirko Milošević to collaborate on this project and helping me in any situation. My thanks belong also to every colleague in the laboratory for advising me whenever needed and being always friendly to me. I must thank also to Jan Brábek and Daniel Rösel for discussing 3D models and Jakub Gemperle for performing experiments, teaching me new methods and bringing a fresh insight into my project.

The study was supported by the Charles University, project GA UK No. 1506318

Abstract

Breast cancer is a common malignant disease affecting millions of women worldwide. Amplification of HER2 oncogene, a tyrosine kinase receptor, in breast cancer allows application of targeted therapy, but approximately one third of patients develop resistance to treatment. Relocalization of HER2 from the plasma membrane into the mitochondria was found and suggested as one of the potential causes of such resistance. Here we document that the function of mitochondrial HER2 is distinct from that of HER2 in the plasma membrane. Mitochondrial HER2 enhances cancer cell energetic metabolism, proliferation and migration *in vitro*, and tumour formation *in vivo* in mice correlating with elevated level of ROS signalling. The kinase activity of mitochondrial HER2 is unaffected, therefore I investigated its role in mitochondrial HER2 function. Moderate, endogenous levels of the kinase activity of mitochondrial HER2 drive pro-tumorigenic properties of breast cancer cells, while constitutive kinase activity sensitizes these cells to cell death and attenuates tumour formation in animal models. On the other hand, impairment of kinase activity due to mutation in the ATP binding site of mitochondrial HER2 supports adherence-independent growth *in vitro* and tumor growth *in vivo*. We propose that HER2 function in mitochondria is partially kinase-dependent, but mitochondrial HER2 also contributes by an additional unidentified mechanism that provides advantage for kinase dead mutants in tumour formation. Last but not least, the kinase activity of mitochondrial HER2 sensitizes breast cancer cells to novel anti-cancer agent MitoTam that is now in clinical trials.

Key words:

HER2, breast cancer, mitochondria, mitochondrial HER2, cancer metabolism, trastuzumab resistance, MitoTam, ROS

Abstrakt

Rakovina prsu je častým nádorovým onemocněním postihující miliony žen po celém světe. Amplifikace onkogenu HER2 v rakovině prsu sice umožňuje nasazení cílené terapie, nicméně až u třetiny pacientek dochází k vytvoření rezistence vůči léčbě. Jeden z možných mechanismů rezistence může být relokalizace HER2, receptoru s tyrosinkinázovou aktivitou, z plazmatické membrány do mitochondrií. Nicméně mechanismus působení mitochondriální frakce HER2 zřejmě nevyužívá kanonickou signalizaci HER2 umístěného v plazmatické membráně. Mitochondriální HER2 zvyšuje energetický metabolismus rakovinných buněk, proliferaci a migraci v několika *in vitro* modelech a tvorbu nádorů v myších spojenou se zvýšenou produkcí ROS. Mitochondriální HER2 je kinázově aktivní, a já jsem se proto zabývala rolí kinázové aktivity v jeho funkci. Kinázová aktivita mitochodnriálního HER2 podporuje některé vlastnosti potřebné v tumorigenezi, ale konstitutivní kinázová aktivita způsobila zvýšenou citlivost buněk k buněčné smrti a zpomalila růst nádorů v myším modelu. Na druhé straně, mutace v ATP-vazebném místě HER2, s níž je HER2 kinázově neaktivní, zvýhodnila buňky v růstu bez možnosti adheze a v tvorbě nádorů *in vivo*. Lze proto navrhnout, že mitochondriální funkce onkogenu HER2 je závislá nejen na jeho kinázové aktivitě, ale také zahrnuje další, dosud neobjasněný mechanismus, který zvýhodňuje buňky nesoucí mitochodnriální HER2 bez kinázové aktivity v tvorbě nádorů. V neposlední řadě jsou buňky s konstitutivní kinázovou aktivitou mitochondriálního HER2 citlivější k látce MitoTam, která je v současné době podrobena klinickému testování.

Klíčová slova:

HER2, rakovina prsu, mitochondrie, mitochondriální HER2, metabolismus rakovinných buněk, rezistence, MitoTam, ROS

List of Abbreviations

AKT	aka PKB (Protein kinase B)
ATP	Adenosine triphosphate
CI-CIV	Complexes of respiratory chain
CoQ	Coenzyme Q
COX8	Cytochrome c oxidase subunit 8
Cyt c	Cytochrome c
DHODH	Dihydroorotate dehydrogenase
ECM	Extracellular matrix
ER	Estrogen receptor
FDG	^{18}F-fluorodeoxyglucose
GLUT	Glucose transporter
GRB2	Growth factor receptor-bound protein 2
GSK-3β	Glycogen synthase kinase 3β
HER1	Human Epidermal Growth Factor Receptor 1, aka EGFR, ERBB1
HER2	Human Epidermal Growth Factor Receptor 2, aka ERBB2
HER3	Human Epidermal Growth Factor Receptor 3, aka ERBB3
HER4	Human Epidermal Growth Factor Receptor 4, aka ERBB4
HKII	Hexokinase II
IMM	Inner mitochondrial membrane
MAPK	Mitogen-activated protein kinase
MCF7	Breast cancer cell line (Michigan Cancer Foundation-7)
MCT1	Monocarboxylate transporter 1
MDA MB 231	Triple-negative breast cancer cell line
mtDNA	Mitochondrial deoxyribonucleic acid
mTORC1	Mammalian target of rapamycin complex 1
MTS	Mitochondrial targeting sequence

NADH	Nicotinamide adenine dinucleotide
NADPH	Nicotinamide adenine dinucleotide phosphate
NDUFA13	NADH dehydrogenase subunit 13, aka GRIM19
NDUFA9	NADH dehydrogenase subunit 9
NRG1	Neuregulin 1
OMM	Outer mitochondrial membrane
OXPHOS	Oxidative phosphorylation
PDK1	3-phosphoinositide-dependent protein kinase-1
PDK2	3-phosphoinositide-dependent protein kinase-2
PET	Positron emission tomography
PFK2	Phosphofructokinase 2
PI3	Phosphatidylinositol triphosphate
PI3K	Phosphatidylinositol triphosphate kinase
PR	Progesterone receptor
PTEN	Phosphatase and tensin homolog
ROS	Reactive oxygen species
SC	Supercomplex
SOD2	Superoxide dismutase 2, aka MnSOD
STAT	Signal transducer and activator of transcription
TCA	Tricarboxyl acid
TPP+	Triphenylphosphonium
VDAC	Voltage-dependent anion channel

Table of Content

1 Introduction

1.1 HER2 – tyrosine kinase from the EGFR family

HER2 (Human Epidermal Growth Factor Receptor 2) also known as ERBB2 is a large (185 kDa) kinase receptor from the family of Epidermal Growth Factor Receptors, localized mainly in the cytoplasmic membrane. It is abundantly expressed in foetal epithelium, while expression in adult tissues is very low (Mori et al., 1989). The name ERBB2 comes from the close similarity to v-erbB (avian erythroblastosis oncogene B). It was first discovered as a rodent orthologue of ERBB2 gene called neu in rat neuroblastomas and is highly homologous to EGFR and other members of ERBB family (Coussens et al., 1985).

At the N-terminus of ERBB2 (Fig. 1.1) there is the extracellular domain (ECD) with cysteine-rich clusters, followed by the transmembrane domain (TMD). The intracellular tyrosine kinase domain (TKD) is highly homologous not only to EGFR and v-erbB but also to SRC kinase family. Studies of kinases in this family uncovered residues Gly727 and Lys753 of HER2 being involved in ATP binding. Gly727 is located into an N-loop, binds ATP, and helps to orient ATP molecule and the substrate. When HER2 is active, Lys753 forms a salt bridge with Glu770 which coordinates phosphatases of ATP bound into an active site. The signal transducing domain (STD) on the C-terminus is less homologous among the family members and contains tyrosine residues standing for autophosphorylation sites (the major one in HER2 is Tyr1248) (Coussens et al., 1985). It was found that mutation of Val659 to glutamine enhances autophosphorylation of HER2 and thus its signalling potential (Akiyama et al., 1991).

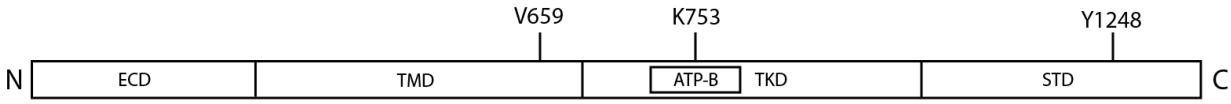

Figure 1.1: ***HER2 scheme:*** *ECD – extracellular domain, TMD – transmembrane domain, ATP-B – ATP-binding site, TKD – tyrosine kinase domain, STD – signal transducing domain*

1.1.1 Heterodimerization and functional interaction between EGFR family members

EGF receptor family (or ERBB family) consists of EGFR (HER1, ERBB1), HER2 (ERBB2), HER3 (ERBB3), and HER4 (ERBB4). Signal transduction from extracellular ligand to intracellular signalling cascades is proceeded by dimerization of these receptors and *trans*-autophosphorylation of crucial tyrosine residues in their signal transducing domains.

Homodimers and heterodimers are both possible. Ligand binding and activation is followed by receptor endocytosis and subsequent recycling or degradation of receptors (Waterman and Yarden, 2001). HER2 does not have extracellular binding site for a soluble ligand, it has a constitutive open formation of extracellular domain and serves as the preferred dimerization partner for other EGFR family members which are ligand-activated. The strongest and most potent interaction is between HER2 and HER3 – a kinase deficient family member (Tzahar et al., 1996). HER3, activator of PI3K/AKT pathway, can be phosphorylated only in heterodimer with another family member. Overexpression of HER2 in cancer leads to excessive activation of HER3 and dimerization of HER2 without ligand resulting in a constitutive activation of HER2 signalling (Hynes and Lane, 2005).

1.1.2 HER2 signalling

HER2 signal transducing domain contains 19 tyrosine residues free for phosphorylation. Eight of them are recognized by specific protein motifs (Schulze et al., 2005). Thus, activated HER2 can interact with many downstream factors and its role in cell maintenance is complex. Number and composition of interacting proteins also differs depending on HER2 dimerization partner (Croucher et al., 2016). Main pathways activated by HER2 signalling are PI3K/AKT, MAPK signalling pathway, WNT, Phospholipase C and STAT transcription factors (Yarden and Sliwkowski, 2001). HER2 can also translocate into nucleus and become a transcription factor itself (Wang et al., 2004). Moreover, nuclear localization of HER2 brings worse prognosis for patients (Schillaci et al., 2012). HER2 signalling promotes cell survival, mitochondrial function, proliferation, cell migration and metabolism (Hynes and Lane, 2005).

1.1.3 HER2 in physiological conditions – signalling in the heart

Physiological HER2 activity is involved in heart and neural development (Britsch et al., 1998; Liu et al., 1998). HER2 signalling in the heart has been broadly studied due to cardiotoxicity of HER2 targeted drugs. HER2 signalling is essential in heart development, tissue maintenance and regeneration.

Signalling through HER2 in the heart is dependent on the presence of NRG1 (Neuregulin 1) – a ligand of HER3 and HER4. HER2 and HER4 are highly expressed prenatally and its expression lowers soon after birth (Odiete et al., 2012). Lack of either HER2,

NRG1, or HER4 leads to death of mouse embryos in utero around day 10 with cardiac development defects (Gassmann et al., 1995; Lee et al., 1995; Meyer and Birchmeier, 1995). In adulthood, NRG1/ERBB signalling axis enables physiological adaptations of cardiac structure and function to changes of demands. The NRG1/ERBB system is activated during physiological overload of heart during pregnancy (Lemmens et al., 2011). It was also found that increased heart failure is associated with lowered expression of HER2 and HER4 leading to elevated susceptibility to apoptosis of myocardial cells (Rohrbach et al., 2005).

1.2 Breast Cancer

1.2.1 Epidemiology

Breast cancer is the most common malignant disease among women (Ferlay et al., 2015). In 2018 over 2 million women were diagnosed with breast cancer worldwide. 5-year prevalence counts over 6.8 million women suffering from this disease. It is estimated that over 626 thousand women died of breast cancer in 2018 (Bray et al., 2018).

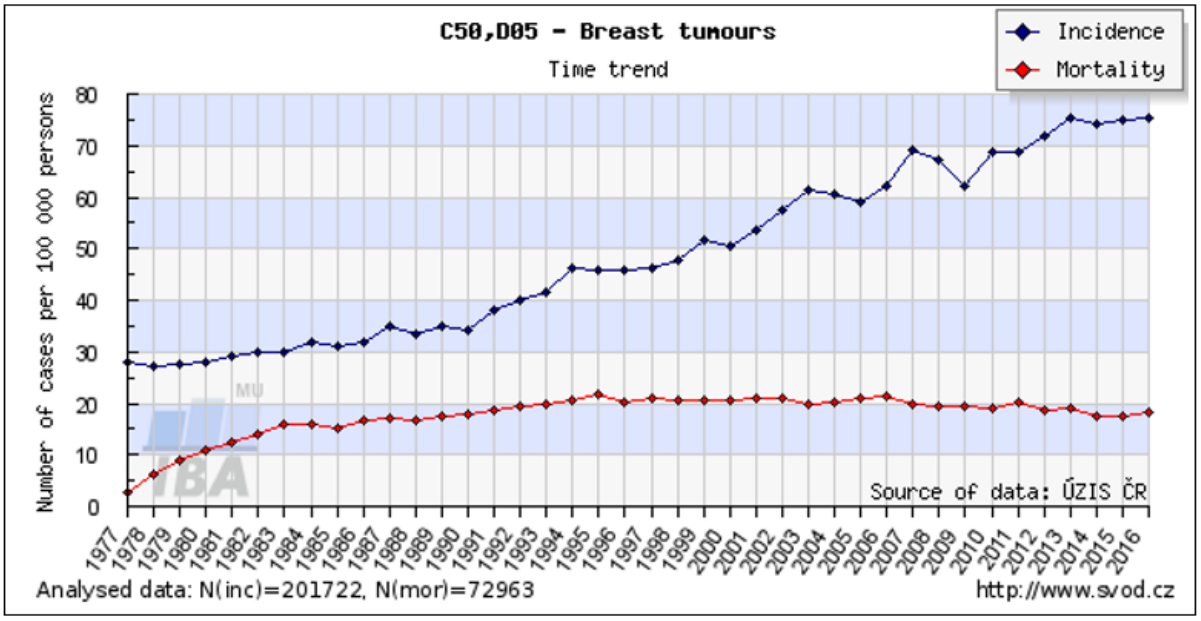

Figure 1.2: ***Incidence and mortality of breast cancer in the Czech Republic.*** *Generated at* www.svod.cz *website (Dušek L., 2019).*

National Oncological Register of Czech Republic returns 7869 women diagnosed and 1921 dead of breast cancer in Czech Republic in 2016. Even though the incidence increases in time, mortality plateaus (Fig. 1.2) (Dušek L., 2019). This discrepancy occurs most probably thanks to improving system of prevention and successful treatment of the early-stage forms.

Five-year survival rate for *in situ* breast cancer is 99 %, whereas presence of metastases decreases it to 27 % (Howlader N., 2017). This rapid drop is mostly caused by the resistance to treatment developed in metastatic form of the disease (Rivera and Gomez, 2010).

1.2.2 Breast cancer subtypes

Historically, definition of various subtypes of breast cancer came from histology. With the emergence of molecular biology, definitions of subtypes were built on expression profile of genes involved in cancer progression which are targetable by treatment. The most important are ER (estrogen receptor), PR (progesterone receptor), Ki-67 – marker of proliferation, and HER2. Here I show definitions reviewed by Expert Panel at the 13th St Gallen International Breast Cancer Conference (Goldhirsch et al., 2013) (Tab. 1.1).

Molecular subtype	Gene expression profile	Therapy
Luminal A	ER+, PR+, HER2-, Ki-67 low	Endocrine therapy is often used alone
Luminal B HER2-	ER+, HER2- *and at least one of:* Ki-67 high, PR- or low,	Endocrine therapy for all patients, cytotoxic therapy for most
Luminal B HER2+	ER+, HER2+, PR-, Ki-67-, PR-	Cytotoxics + anti-HER2 + endocrine therapy
HER2 positive	ER-, PR-, HER2+	Cytotoxics + anti-HER2 therapy
Basal like	„triple negative" – ER-, PR-, HER2-	Cytotoxics

Table 1.1: ***Types of breast cancer:*** *Adopted from (Goldhirsch et al., 2013).*

1.2.3 HER2 positive breast cancer

It is more than thirty years since the association of HER2 amplification with human breast cancer progression has been established (King et al., 1985; Slamon et al., 1987). Even though HER2 and its effects in cancer has been massively studied since its discovery and the anti-cancer drugs targeting HER2 came into clinical usage, HER2 positive breast cancer is often connected with relapses, resistance to treatment and overall poor prognosis for patients (Hynes and Lane, 2005).

About 15-20 % of breast cancers are HER2 positive. Overexpression is measured immunohistochemically, amplification of *HER2* gene is evaluated by fluorescence in-situ hybridization. Unfortunately, HER2 is the only prognostic marker for targeted therapy. Although patients carrying mutations in related factors such as PI3K or PTEN might benefit

from anti-HER2 treatment, such diagnostics has not yet entered routine clinical practice and patients might not get proper treatment (Loibl and Gianni, 2017).

HER2 was historically seen as a negative prognostic marker. However, targeted therapy brought light into $HER2^{high}$ breast cancer treatment. As a pioneer, Trastuzumab (Herceptin) came first into clinical practice and several HER2 targeting drugs followed (Tab 1.2). Targeted therapy is usually combined with traditional chemotherapeutics, many possible combinations has been studied and the final treatment is settled according to the stage of the disease and patient condition (Loibl and Gianni, 2017).

Anti-cancer drug	Class	Mechanism of action
Trastuzumab	Monoclonal antibody	Binds to extracellular domain, inhibits HER2 and HER3 signalling, and might trigger antibody-dependent cellular cytotoxicity.
Lapatinib	Tyrosine kinase inhibitor	Binds to the intracellular ATP-binding pocket of HER2 and prevents autophosphorylation and downstream signalling.
Pertuzumab	Monoclonal antibody	Antibody directed at the dimerization domain of HER2, prevents heterodimerization with HER3.
Trastuzumab emtansine	Antibody-drug conjugate	Inhibitor of microtubules – emtansine is conjugated by stable linker to trastuzumab.
Neratinib	Tyrosine kinase inhibitor	Tyrosine kinase inhibitor of HER1, HER2 and HER4

Table 1.2: ***Drugs targeting HER2*** *(Loibl and Gianni, 2017; Schramm et al., 2015)*

As previously mentioned, HER2 plays a role in hearth development and maintenance. Thus, long-term anti-HER2 therapy leads to cardiotoxicity (Loibl and Gianni, 2017). Moreover, 70 % $HER2^{high}$ cancer patients develop resistance to targeted treatment (Schramm et al., 2015; Vogel et al., 2002). To overcome this resistance, different variations of combined therapy have been tested. However, further studies of resistance origin and new targeted drugs are needed.

1.3 Hallmarks of cancer

In 2000 Hannahan and Weinberg presented a review article titled 'Hallmarks of cancer' (Hanahan and Weinberg, 2000), which tried to cover the main aspects of cancer cell behaviour. In a 2011 update they extended cancer cell features ending up with ten hallmarks of cancer (Fig. 1.3) (Hanahan and Weinberg, 2011). With this picture I would like to emphasize the complexity of cancer progression even though I can cover only some aspects in my study. It is important not to forget that cancer is caused by many connected events both within cell and on the level of the whole tissue. Hopefully, such complex disease as cancer will be treated by complex approach in near future comprising personalized diagnostics and therapy. In following paragraphs, I focus on cancer hallmarks relevant to my interests.

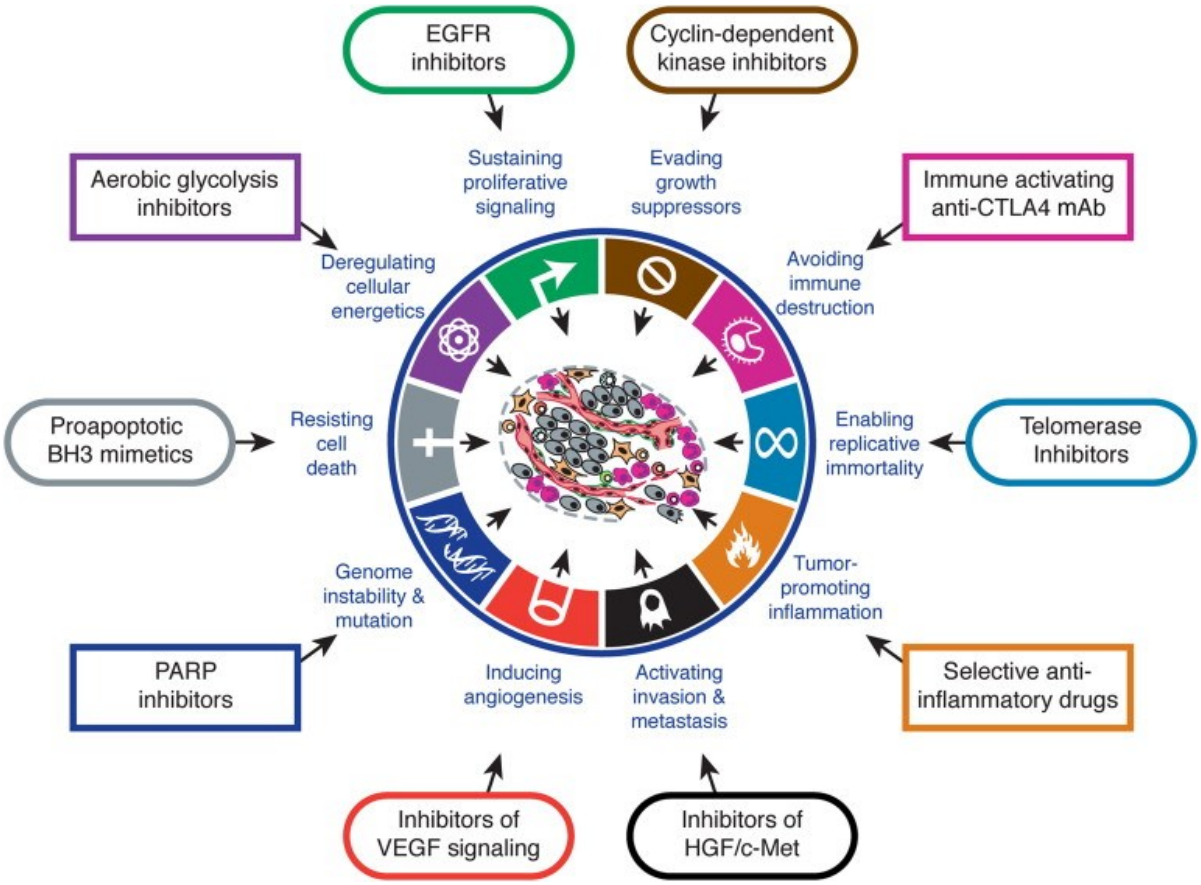

Figure 1.3: ***Ten hallmarks of cancer targetted with illustrative examples of clinically used or developing treatment****. Adopted from (Hanahan and Weinberg, 2011).*

1.3.1 Cancer metabolism

In 1924 Otto Heinrich Warburg postulated that cancer cells can process large amount of glucose into lactate even when oxygen is abundant. Warburg hypothesized that aerobic

glycolysis is a consequence of mitochondrial failure and described fermentation to be a cause of tumour formation (Warburg, 1924; Warburg, 1956). The Warburg's effect was proved to be present not only in cancer cells, but also in every rapidly proliferating cell type. However, now we know that it is not the cause of malignancy, it is just one of the cancer hallmarks. High glucose consumption is beneficial for visualization of tumours in diagnostics – ^{18}F-fluorodeoxyglucose is utilized mainly in cancer cells and its accumulation is pictured through positron emission tomography (FDG-PET) (Fig. 1.4) (Vander Heiden et al., 2009).

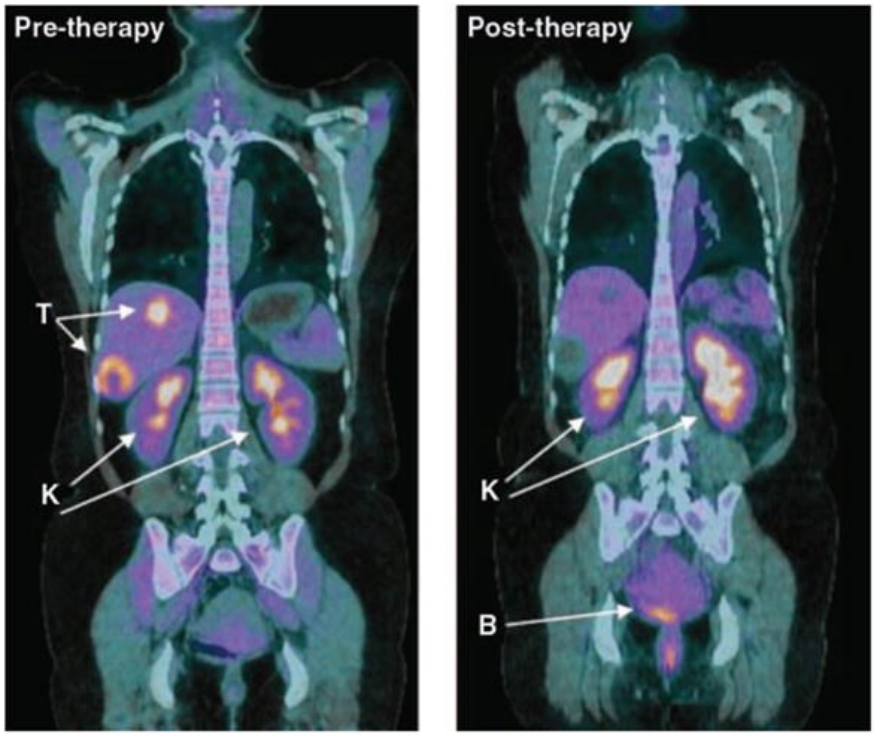

Figure 1.4: ***Positron emission tomography****: High glucose consumption observed in tumour and, being excreted, in kidneys and bladder. Adopted from (Vander Heiden et al., 2009).*

Even though glycolysis followed by lactate production is inefficient in ATP synthesis compared to oxidative phosphorylation (OXPHOS), it provides building stones for anabolic processes and cell growth. In proliferating cells, demand for synthesis of lipids, nucleotides and amino acids is higher than demand for ATP production. Secondary, if product of glycolysis is utilized in TCA cycle and respiratory chain to produce ATP, high level of ATP would inhibit further glycolysis, which is undesirable in proliferating cell (Vander Heiden et al., 2009). Cancer cells utilize glucose and glutamine, but excrete most of it as lactate and alanine, respectively. Demands for energy supply (in case of glucose) or nitrogen supply for

nucleotides synthesis (in case of glutamine) are lesser than demands for NADPH (DeBerardinis et al., 2007). NADPH is required as an electron donor in anabolic reactions. The figure 1.5 pictures connections among glycolysis, glutamine metabolism and the pentose phosphate pathway – main source of NADPH in proliferating cells. Analogically to glucose, glutamine can be also used for positron emission tomography – it is useful in visualizing gliomas as even healthy brain tissue utilizes high amount of glucose. Glutamine shows low background brain uptake unlike glucose (Venneti et al., 2015).

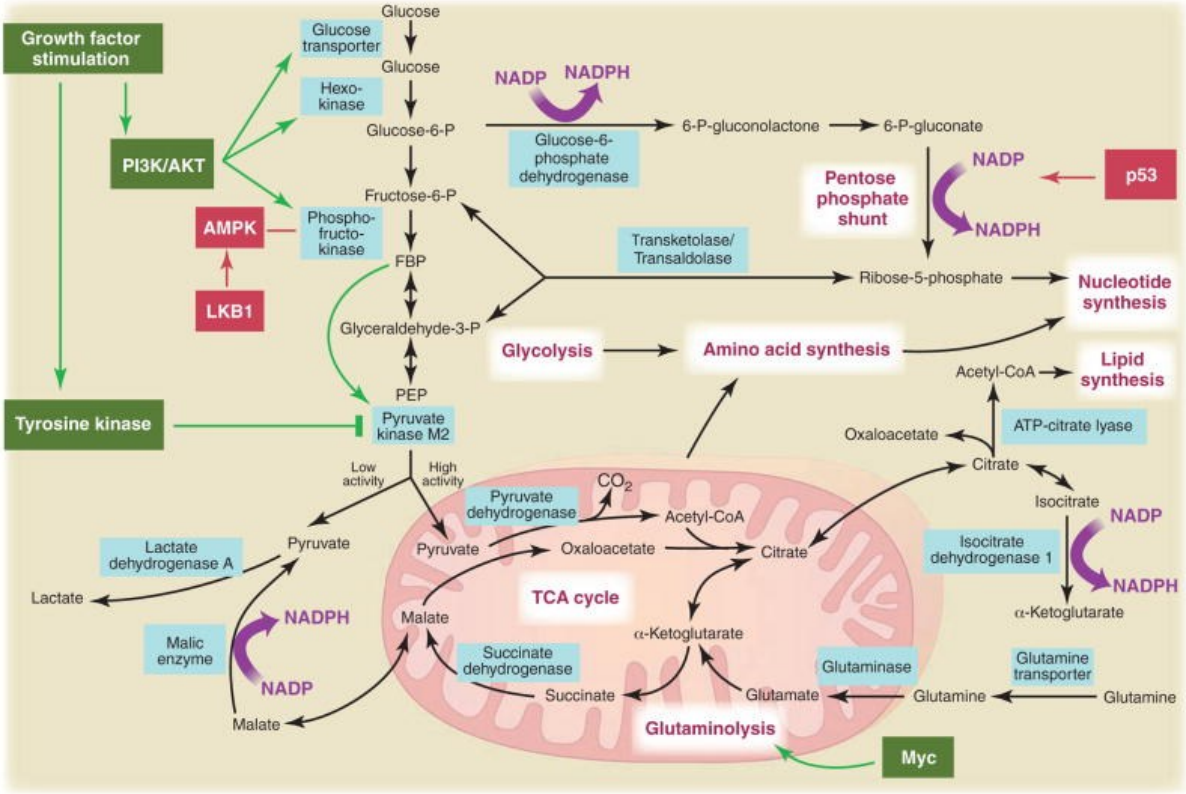

Figure 1.5: ***Cancer metabolism is altered to produce NADPH and building blocks for anabolic reactions.*** *Adopted from (Vander Heiden et al., 2009).*

The Warburg effect is not a result of mitochondrial disorder, it is rather a regulated metabolic state and requires functional mitochondria. Even when energy production in cancer cells does not rely on OXPHOS, mitochondrial function is still essential for tumorigenesis. It has been long known that cells without mitochondrial DNA (mtDNA) show higher susceptibility to cytotoxic drugs and fail to grow in an anchorage-independent manner (Cavalli et al., 1997). When injected into mouse, cells without mtDNA feature a delay in tumour formation compared to control cancer cell line with unaffected mitochondria.

Eventually, even cells without mtDNA can form tumours, invade and progress into metastases due to horizontal transfer of healthy mitochondria from tumour stroma cells. This study shows importance of OXPHOS in tumorigenicity and plasticity that cancer cell exhibit (Tan et al., 2015). However, ATP generation in OXPHOS is not the step affecting tumorigenesis in mtDNA depleted cells. Cells lacking mtDNA are auxotrophic for uridine in culturing medium (Morais et al., 1994). It is because pyrimidine biosynthesis is linked to functional OXPHOS through DHODH (dihydroorotate dehydrogenase) enzyme, the activity of which depends on ubiquinone recycling in the respiratory chain (Bajzikova et al., 2019).

Functional respiration of cancer cells is useful also for another reasons. Tumours are heterogeneous – even though all tumour cells can originate from a single clone, they acquire distinct roles during tumour formation. Ill-formed, chaotic vasculature around tumour leads to uneven conditions. Some cells are supplied by enough oxygen and nutrients while other suffer from shortages. Highly proliferating and metastatic cells show glucose dependency and elevated lactate production. However, there are also supportive cells that use lactate as source of energy and exhibit high respiratory rates. MCT1 – a lactate importer was present only in aerobic parts of tumour biopsies and targeting MCT1 affected tumour growth in mice. Lactate-consuming cells after inhibition of MCT1 utilize glucose instead, leading to glucose deprivation of hypoxic cells (Sonveaux et al., 2008).

1.3.2 Migration and metastasis

More than 90 % of patient mortality is not due to the primary tumour but because of the metastases (Talmadge and Fidler, 2010). Cancer cells can be very plastic and invade any organ in the body. The process is called metastatic cascade (Jiang et al., 2015). Fortunately, only minority of cells has properties to finish the metastatic cascade. Neither motility, nor invasion capability is sufficient for metastasis. It should be highlighted that if an invasive cell cannot complete any of the subsequent steps in the metastatic cascade, it cannot form a metastasis (Welch and Hurst, 2019).

The metastatic potential of cancer is set long before detecting a primary tumour. Already in 1889, Stephen Paget postulated "seed and soil" hypothesis supported by the fact that some tissues (bone, liver, lungs, brain) are preferentially colonized, while other are just rarely invaded (heart, spleen) (Paget, 1889). Being a good soil for cancer cell is not a passive

attribute, tumours communicate with the rest of the body to establish a premetastatic niche (Kaplan et al., 2006).

At the beginning of the metastatic cascade, a subset of cells in primary carcinoma invades through the basal membrane into the underlying stroma. Secondly, invading cells intravasate the vasculature and enter the blood stream. However, the efficiency of dissemination of circulating cells is very low. Cancer cells in the blood stream suffer from the loss of extracellular matrix (ECM) support and sheer stress. Thus, the efficiency of metastases is increased when cells form an emboli – clusters of circulating tumour cells that have 23 to 50-fold higher metastatic potential than single cell counterparts (Aceto et al., 2014).

After extravasation, cancer cells colonize the secondary sites. Disseminated cancer cells still do not have to form metastases, most of them stay dormant. To the Paget's "seed and soil" hypothesis we need to add one more factor – something like a climate. It stands for the patient condition, immune system function, genetic and epigenetic programs, metabolism etc. (Aguirre-Ghiso and Sosa, 2018; Welch and Hurst, 2019).

1.3.3 HER2 proliferative signalling in cancer

HER2 is rarely mutated in breast cancer, it potentiates malignancy through its overexpression, which is associated with increased phosphorylation and activation of PI3K/AKT signalling (Ram and Ethier, 1996). However, HER2 itself is unable to activate this pathway, it requires dimerization partner – HER3. HER3 is often co-expressed with HER2 in breast cancer and HER3 expression leads to worse prognosis. It is a main regulator of PI3K/AKT pathway among ERBB family and translocated into nucleus serves as a pro-proliferative transcription factor (Hsu and Hung, 2016).

HER3 can be activated ligand-independently when HER2 is overexpressed. Obviously, HER2 and HER3 create a close partnership in cancer progression. Downregulation of both HER2 and HER3 decreases proliferation and survival of cells. Although oncogenic potential of HER3 is dependent on HER2 expression, HER3 brings resistance to both hormonal and targeted clinical approaches and thus it is a hot target for cancer therapy (Mishra et al., 2018).

Phosphorylated HER3 contains docking sites for the p85 adaptor unit of PI3K. PI3K activity generates PI3 (phosphatidylinositol triphosphate), a second messenger needed for partial activation of AKT through phosphorylation on Thr308 by PDK1. Fully activated AKT

is also phosphorylated on Ser473 by PDK2 (Fig. 1.6). AKT activation influences many pathways of cell fate including protein synthesis (mainly through mTORC1), survival (through inhibition of p53 and modulating mitochondrial apoptotic pathway), proliferation and glucose metabolism (enhances glucose transport, glycolysis and glycogen synthesis) (Osaki et al., 2004).

Residual HER2-driven activation of PI3K/AKT pathway was recently found even in the absence of HER3 provided by weak binding of PI3K to phosphorylated Tyr1139 of HER2 or indirectly by GRB2 or RAS mediators. It was shown that HER2 can overcome HER3 dependency (Ruiz-Saenz et al., 2018).

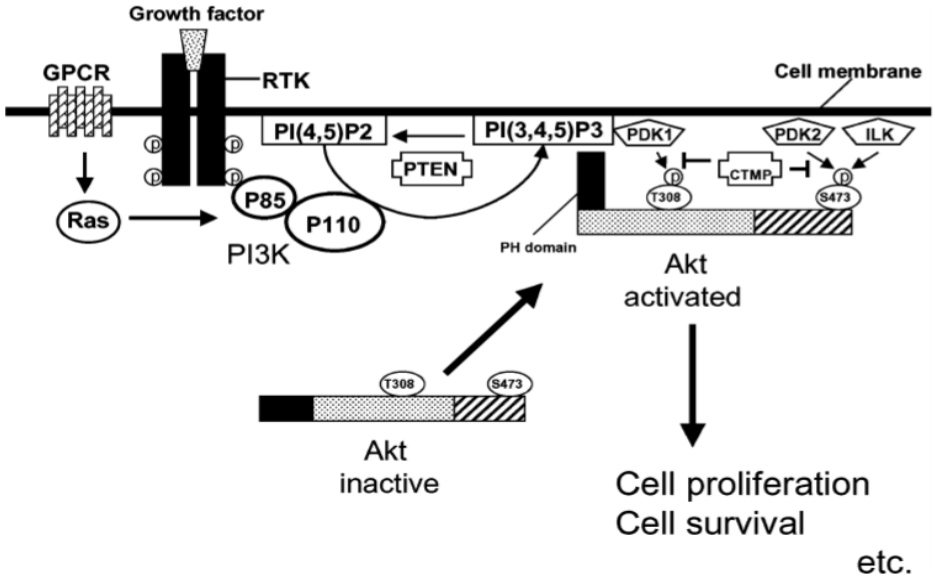

Figure 1.6: ***AKT activation by tyrosine receptor kinase.*** *Adopted from (Osaki et al., 2004)*

The effect of AKT activity is often enhanced by inhibition of PTEN – phosphatase which reduces the amount of IP3. PTEN deficiency in breast cancer leads to resistance to treatment with trastuzumab *in vitro* and *in vivo.* Such engagement of AKT into cell proliferation and survival makes PI3K/AKT pathway a target for anticancer drugs (Nagata et al., 2004).

As the PI3K/AKT pathway is responsible for insulin signalling in physiological conditions, it is a major regulator of glucose metabolism and contributes to the Warburg's effect. PI3K/AKT signalling promotes glucose transporter GLUT1 expression and localization to the membrane (Barthel et al., 1999). This pathway also potentiates glycolysis enzymes activity – AKT activates PFK2 (phosphofructokinase 2) which positively regulates glycolysis

(Deprez et al., 1997). Furthermore, it reactivates expression of embryonic hexokinase II (HKII) which localizes to the outer mitochondrial membrane through interaction with VDAC. Like this, HKII can effectively phosphorylate glucose thanks to constitutive supply of ATP from mitochondria. Moreover, bound to VDAC, HKII hinders binding of pro-apoptotic Bax and Bad into mitochondrial membrane and thus prevents cell death (Mathupala et al., 2006).

GSK-3β is negatively regulated by AKT phosphorylation. Active GSK-3β contributes to degradation of Mcl-1 anti-apoptotic protein (Maurer et al., 2006) and prevents HKII binding to VDAC by VDAC phosphorylation (Pastorino et al., 2005). Due to these mechanisms, AKT provides anti-apoptotic signalling.

1.4 Mitochondria

Mitochondria are semiautonomous organelles standing in the centre of energetic metabolism of every eukaryotic cell. Each consists of two membranes (outer – OMM and inner - IMM) which create highly flexible mitochondrial reticulum. Outer membrane is permeable for small molecules, while inner membrane transport is strictly regulated resulting in establishment of a membrane potential. In the IMM there are four complexes of respiratory chain using reduced coenzymes from catabolic reactions as electron donors. During transport of electrons through respiratory chain, protons are translocated from the mitochondrial matrix into the intermembrane space. ATP synthase exploits membrane potential of protons to generate ATP. This process of energy conversion is termed oxidative phosphorylation (OXPHOS) (Mitchell, 1961; Saraste, 1999).

1.4.1 Supercomplexes

Respiratory chain consists of four complexes. The first two, CI and CII, accept electrons from NADH and succinate, respectively. Electrons are further transferred to mobile Coenzyme Q (CoQ) which docks to complex III, where another mobile element, cytochrome c, accepts electrons and passes them to complex IV. Final acceptor is atomic oxygen and water is produced. There was a long debate about the structure and function of respiratory chain. In the middle of the 20th century a "solid state" model was postulated – respiratory components are tightly packed into rigid structures that efficiently transport electrons (Chance and Williams, 1955; Slater, 2003). Later, it was proposed that complexes of respiratory chain and corresponding mobile elements diffuse in the IMM and pass the electrons in

random collisions (Hackenbrock et al., 1986). However, with establishing of the blue native electrophoresis method allowing co-migration of interacting mitochondrial proteins (Schägger and von Jagow, 1991; Wittig et al., 2006), higher structures, supercomplexes (SCs), were observed (Schägger and Pfeiffer, 2000). Currently, a "plasticity model" connecting both previous hypothesis describes dynamic equilibrium between freely diffusing forms and supercomplexes (Acin-Perez and Enriquez, 2014).

Respirasome is a supercomplex comprising all partners required for transfer of electrons from NADH to oxygen. It consists if complex I, dimer of complex III and at least one molecule of complex IV (SC I+III_2+IV). Additionally, SC I+III_2 and SC III_2+IV_{1-2} are both possible (Acin-Perez and Enriquez, 2014). Higher supercomplex organization elevates respiration rate (Lapuente-Brun et al., 2013) and protects respiratory complexes from reactive oxygen species (ROS) generation (Lopez-Fabuel et al., 2016).

1.4.2 ROS production

Respiratory chain reduces oxygen to water. Partial reduction of oxygen molecule leads to the production of a by-product, reactive oxygen species (ROS). As no mechanism is 100% efficient, every cell can handle basal ROS production by antioxidants expression in both mitochondria and cytosol. However, cancer cells feature higher level of ROS, sometimes even followed by low antioxidant defence. Oxidative damage affects all structures - proteins, lipids and nucleic acids, leading to genetic instability and tumorigenesis. ROS promote malignancy not only by their high potency for oxidative damage but also through signalling contributing to abnormal cell growth, metastasis, angiogenesis, and resistance to apoptosis. However, excess level of ROS leads to cell death even in tumour cells (Fig. 1.7). Thus, manipulating ROS production is a promising mean to new anti-cancer treatment (Moloney and Cotter, 2018).

The most potent ROS, superoxide $O_2^{\bullet -}$ and hydrogen peroxide H_2O_2, are produced mainly by complex I, II and III of the respiratory chain. $O_2^{\bullet -}$ is dismutated by MnSOD (SOD2) into H_2O_2 which serves as a second messenger to various targets. Antioxidants including catalase, the glutathione system, peroredoxins, and thioredoxins maintain H_2O_2 levels by reduction to H_2O (Moloney and Cotter, 2018). ROS inactivate PTEN phosphatases responsible for tyrosine dephosphorylation. Thus, PI3K/AKT pathway is triggered leading to pro-proliferative and anti-apoptotic signaling (Leslie et al., 2003).

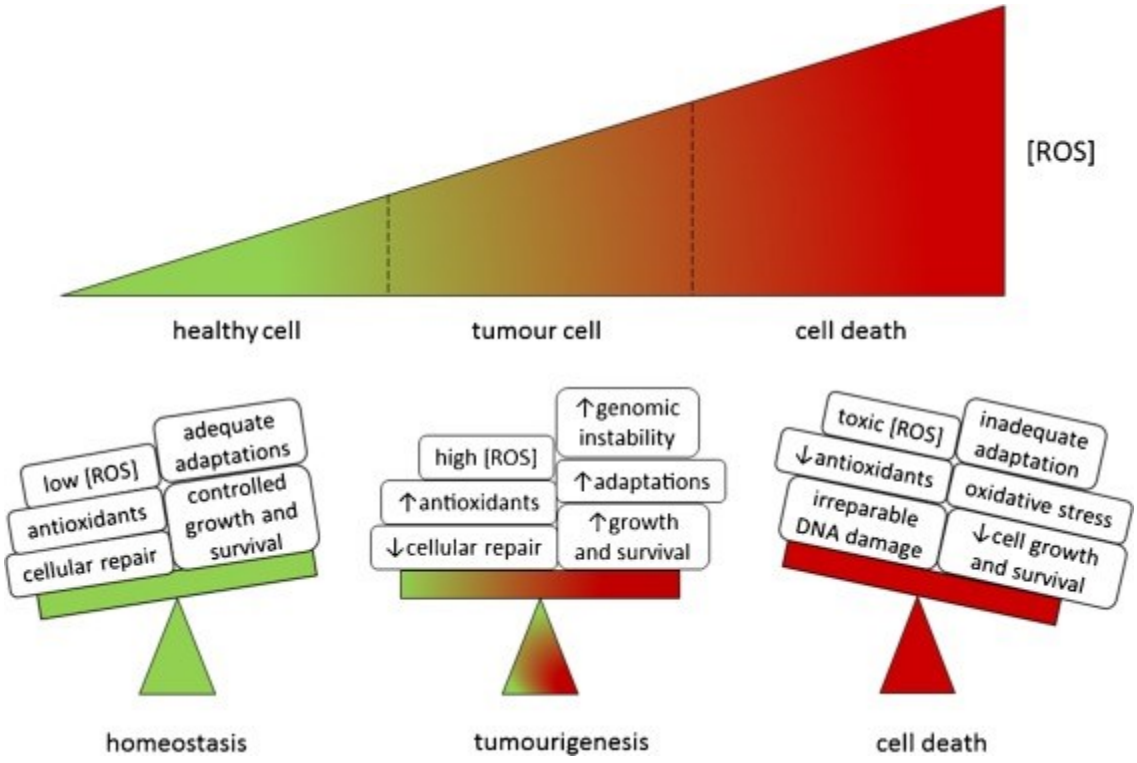

Figure 1.7: ***ROS production signalling changes with its level.*** *Adopted from (Moloney and Cotter, 2018).*

1.5 Mitochondrially targeted proteins – what is not in Mitocarta

Targeting proteins into mitochondria is a regulated process. Mitocarta 2.0, catalogue of genes encoding canonical mitochondria-targeted proteins, contains to date 1158 human genes (Calvo et al., 2016). Products of these genes are localized into mitochondria among several healthy tissues. However, cancer cells were not classified and they often feature reorganizations. Amplification of oncogenes also facilitates its spread among organelles. Thus, mitochondria of cancer cells are inhabited by various proteins not observed in healthy tissues.

As an example there is a fraction of estrogen receptor (ER) found in mitochondria in MCF7 cell line supporting cell survival (Pedram et al., 2006). Furthermore, Mdm2 oncoprotein was found in mitochondria of breast cancer cells with p53-independent function. Mitochondrial Mdm2 regulates activity of complex I and increases cancer cell invasion and migration (Arena et al., 2018). On the contrary, p53 translocation into mitochondria initiates apopotosis (Mihara et al., 2003).

More interestingly, even members of the EGFR family were observed in mitochondria. EGFR translocates into mitochondria in a manner dependent on its catalytic activity and mitochondrial targeting sequence was found in the juxtamembrane region of EGFR (Demory et al., 2009). In some breast cancer cell lines and also in later-stage breast cancer, simultaneous co-overexpression of EGFR and c-Src was observed. MDA MB 231 cells overexpressing both EGFR and c-Src displayed elevated tumorigenicity in nude mice (Biscardi et al., 1998). When EGFR is phosphorylated on Tyr845 by c-Src, it interacts in mitochondria with COXII, a subunit of complex IV. EGF stimulation of EGFR in c-Src overexpressing cells led to complex IV activity decrease and a drop of ATP production. However, when mutated EGFR without mitochondrial targeting sequence was expressed, ATP level was restored (Demory et al., 2009).

Another member of EFGR family, HER4, undergoes a proteolytic cleavage after activation and the resulting intracellular domain, 4ICD, serves as a BH3-only protein affecting regulation of apoptosis initiation. Interaction of 4ICD with BCL-2 triggers apoptosis of breast cancer cells treated by tamoxifen, an ER-targeted anticancer therapeutic. Thus, the loss of HER4 expression might be a cause of resistance to tamoxifen treatment (Naresh et al., 2008).

1.5.1 HER2 in mitochondria

Last but not least, mitochondrial localization of HER2 was observed. HER2 was found in mitochondria of HER2-transfected cells, cells expressing endogenous HER2 and in patient-derived samples. HER2 contains endogenous mitochondria targeting sequence in transmembrane and membrane-flanking domains. Amino acids 623-689 are necessary and sufficient for mitochondrial localization of HER2 (Ding et al., 2012). HER2 enters mitochondria via mtHSP70 and localizes into inner mitochondrial membrane (IMM) (Ding et al., 2012; Rohlenova et al., 2017)

For further study Ding and colleagues (2012) produced HER2 fused with MTS from complex IV to enrich mitochondrial fraction of HER2, and HER2 lacking internal MTS unable to localize into mitochondrial membrane (HER2-dMTS). These constructs were overexpressed in MDA MB 231 cell line. They observed suppressed oxygen consumption in cells with HER2-MTS, while respiration of cells with HER2-dMTS was not affected. On the other hand, HER2-MTS overexpression enhanced glucose uptake and lactate production

compared to wild-type (WT) and dMTS variant suggesting that mitochondrial HER2 switches metabolism of cancer cells from respiration to glucose utilization (Ding et al., 2012).

Ding et al. (2012) also showed increased resistance of MTS-HER2 expressing cells to trastuzumab (Herceptin). They suggested that internalization of HER2 into mitochondria hides the receptor from trastuzumab, sustaining HER2 signalling. Supporting this hypothesis, they observed elevated mitochondrial localization of HER2 in BT474 cells after trastuzumab treatment (Ding et al., 2012). If HER2 translocation into mitochondria is confirmed as cause of resistance to Trastuzumab, mitochondrial HER2 evaluation could become a good method in diagnostics supporting personalized medicine.

In our laboratory a promising anticancer agent has been synthesized and tested. It is named MitoTam, which stands for mitochondrially targeted tamoxifen. Attachment of triphenylphosphonium (TPP+) group to tamoxifen leads to its accumulation inside mitochondria and impairment of respiratory chain function. Unlike tamoxifen, MitoTam is very effective in killing $HER2^{high}$ breast cancer independently on the canonical HER2 signalling. It induces mitochondrial ROS production particularly in $HER2^{high}$ cells. Furthermore, it was found that MitoTam affects complex I activity and disrupts assembly of respiratory supercomplexes. Localization of HER2 into the inner mitochondrial membrane was also observed in this study. $HER2^{high}$ MCF7 cells without mtHSP70, unable to transport HER2 into mitochondria, were less susceptible to MitoTam then their MCF7 $HER2^{high}$ counterparts. Consistently, MCF7 cells expressing HER2-MTS were more sensitive to MitoTam than cells with HER2-WT or HER2-dMTS leading to a conclusion that mitochondrial HER2 pool determines susceptibility to MitoTam (Rohlenova et al., 2017). These days MitoTam is in phase 1b of clinical trials and hopefully will become a new targeted treatment in $HER2^{high}$ breast cancer.

2 Aims

The aim of this study is to deepen the knowledge about mitochondrial HER2 in breast cancer cells and evaluate the role of its kinase activity in its function. I will focus on evaluating metabolism of cells with variants of mitochondrial HER2, their tumorigenicity and sensitivity to cell death. Here I would like to formulate three main questions:

What is the function of mitochondrial pool of HER2 in breast cancer?

Is the function of mitochondrial HER2 dependent on its tyrosine kinase activity?

Does tyrosine activity of mitochondrial HER2 sensitize cells to MitoTam?

3 Materials and Methods

All chemicals and material were purchased from Sigma Aldrich or stated otherwise.

3.1 Experimental model preparation

MDA MB 231 cell line was obtained from J. A. López (Griffith University, Australia) and authenticated using STR analysis. Cell lines carrying HER2-WT and HER2-MTS were already available (Rohlenova et al., 2017). To study the role of kinase activity of mitochondrial HER2, I prepared kinase mutants of HER2-MTS. K753M is a mutation in ATP-binding site of tyrosine kinase domain leading to kinase deficiency of HER2-MTS. On the other hand, I used mutation V659E leading to constitutive kinase activity (see introduction).

3.1.1 Quikchange site directed mutagenesis

Into PCR reaction, I put vector pEF/IRES/Puro with HER2-MTS and primers targeted into place of mutation required and carrying two-nucleotide mutations leading to K753M or V659E phenotype.

Reaction:

100 ng	DNA
0.8 µl	10uM dNTP (Fermentas, R0241)
1 µl	primers (F+R 10uM)
0.4 µl	Q5-DNA pol (New England Biolabs, M0491L)
8 µl	GC enhancer (New England Biolabs, B9028A)
8 µl	Q5pol buffer (New England Biolabs, B9027S)
x µl	dH2O
Total:	40 µl

PCR program:

1 min	98°C	
10 s	98°C	25x
30 s	55°C	
7 min	72°C	
2 min	72°C	

Primers (mutation underlined):

HER2-MTS V659E F

5'-GACCAGCAGAATGCCCTCCACCGCAGAGACGA-3'

HER2-MTS V659E R

5'-TCGTCTCTGCGGTGGAGGGCATTCTGCTGGTC-3'

HER2-MTS K753M F

5'-GATGTGTTTTCCCTCAACACCATGATGGCCACTGGAATTTTC-3'

HER2-MTS K753M R

5'-GAAAATTCCAGTGGCCATCATGGTGTTGAGGGAAAACACATC-3'

The template vector was degraded by DPN I (Thermo Fisher Scientific, FD1704), which cleaves methylated DNA (1 µl DPN I/20 µl reaction, 30 min 37°C, 5 min 80°C).

3.1.2 Bacteria transformation

TOP10 bacteria genotype C404003 (ThermoFisher) (F- *mcrA* Δ(*mrr-hsd*RMS-*mcr*BC) Φ80*lac*ZΔM15 Δ *lac*X74 *rec*A1 *ara*D139 Δ(*araleu*)7697 *gal*U *gal*K *rps*L (StrR) *end*A1 *nup*G)

Competent TOP10 bacteria were transformed with the PCR product. 5 µl from QuikChange reaction was incubated with competent TOP10 bacteria for 20 minutes, after 45s 42°C heat shock bacteria were incubated for 2 minutes on ice and then grown in 1 ml of LB medium (LB Broth Miller, Amresco). After 1 hour bacteria were centrifuged and seeded on agar plates. Thanks to resistance to ampicillin carried by the vector, I could select colonies of transfected bacteria. Presence of HER2 in the bacterial plasmid was first checked by colony PCR.

Colony PCR mix	**final concentration**
2x Mastermix Dream Taq (Thermo Fisher Scientific, K1081)	1x
primers F/R 10µM	0.2µM
DMSO (D2650)	5%
10% Tween 20 (P7949)	0.10%
H2O	
Final volume	15 µl

PCR program:

3 min	95°C	
30 s	94°C	35x
30 s	65°C	
70 s	72°C	
4 min	72°C	

Primers

Forward: 5′-ATAAAGCTAGCCTCGAGCACCATGGAGCTGGCGG-3′

Reverse: 5′-ATAAATCTAGAGAATTCTCACACTGGCACGTCCAGAC-3′

Products were separated in 1% agarose gel with 1:10 000 GelRed (Biotium, 41003). In case of positive clones, I used NucleoSpin Plasmid kit (Macherey-Nagel, 740499.250) to isolate vector from bacteria and checked presence of the mutation by Sanger sequencing performed by GATC Company. Positive clones were further amplified, stored in glycerol stocks (30% glycerol in LB medium) and DNA for cancer cell transfection was isolated using NucleoBond Xtra Midi kit (Macherey-Nagel, 740410.100).

3.1.3 Cancer cell line transfection

MDA-MB-231 cell line was transfected with DNA constructs using Lipofectamin 3000 Transfection Reagent (Invitrogen, L3000008) and Opti-MEM medium (Thermo Fisher Scientific, 31985070) following recommended protocol. 400 thousand cells were plated into 6-well plate and transfected after 24 hours using 2 µg of DNA. Transfected cells carry Puromycin resistance. Thus, after 24 hours from transfection, cells were selected with Puromycin. Growing in selection medium with 0.25µg/ml Puromycin (InvivoGen, ant-pr), colonies originating from single cell with incorporated vector were formed. Individual colonies were collected and tested for HER2 expression by western blotting. Selected clones were further cultivated in lower concentration of Puromycin (0.12 µg/ml).

3.2 Cell culturing

All cell lines were cultivated in DMEM (D6429) with 10% FBS (F7524), 100 U/ml Penicillin (P3032) and 100µg/ml Streptomycin (S9137) in 37°C and 5%CO_2. Transfected cell lines were cultivated in media with Puromycin (0.12 µg/ml, InvivoGen, ant-pr). For experiments, I always used medium without Puromycin to provide the same conditions for

all cell lines. Cells were passaged every 2-3 days using trypsin solution (0.25% trypsin, 0.01% EDTA). For cell counting I used CASY Cell Counter Model TT (Roche Innovatis AG). Cells were cultivated in NUNC plastic (ThermoFisher) if not stated otherwise.

3.3 SDS-PAGE and Western Blotting

Solutions:

RIPA buffer	20mM TRIS, pH 7,5, 150mM NaCl, 1mM EDTA, 1mM EGTA, 1% NP- 40, 0.1% SDS, 0.5% sodium deoxycholate
4x Sample buffer	40% glycerol, 260mM TRIS, pH 6.8, 8% SDS and 200mM DTT in dH_2O and a whit of bromphenol blue (B0126)
Running buffer	25mM TRIS, 130mM Glycine, 0.1% SDS in dH_2O
Transfer buffer	25mM TRIS, 117mM Glycine, 20% methanol in dH_2O
TBS/Tween	20mM TRIS, pH 7.6, 137mM NaCl, 0.05% Tween 20 (P7949)
10% Separating gel	380mM TRIS, pH 8.8, 10% BAA (Bisacrylamide, Bio-Rad, 1610156), 0.1% SDS, 0.1% APS (ammonium persulfate), 0.1% TEMED (T9281) in dH_2O
Stacking gel	125mM TRIS, pH 6.8, 4% BAA, 0.1% SDS, 0.1% APS (ammonium persulfate), 0.1% TEMED in dH_2O

Antibodies used:

HER2 antibody (SAB4300350), Beta-Tubulin antibody (T4026), HSP60 antibody (Cell Signaling, 12165), Secondary anti-mouse antibody (Bio-Rad, 170-6516), Secondary anti-rabbit antibody (Thermo Fisher Scientific, 15140)

Cells were scraped and lysed in RIPA buffer with protease inhibitors (Serva, 39102.01). Solution was cleared by centrifugation and its concentration measured using BCA Protein Assay Kit (Thermo Fisher Scientific, 23225). Samples were diluted obtaining same concentration in each sample, mixed with 4x Sample buffer and heated for 5 min at 98°C.

SDS-PAGE and Western blotting were performed according to standard protocols (Kurien and Scofield, 2006; Laemmli, 1970). Samples were loaded together with the protein standards into 10% polyacrylamide gel and run in Running buffer at constant 35 mA per gel. Wet western blotting was performed after SDS-PAGE using nitrocellulose membrane (Bio-Rad, 1620115) and Transfer buffer. Membrane was blocked in 5% skimmed milk (Serva,

42590.02) in TBS/Tween and incubated with primary antibody (in 1% milk) overnight. After washing in TBS-Tween, membranes were incubated with secondary antibody for 1h, washed again and proteins were visualized using ECL Western Blotting Substrate (Thermo Fisher Scientific, 32106) or SuperSignal West Femto Maximum Sensitivity substrate (Thermo Fisher Scientific, 34096). Pictures were obtained by CCD Azure Biosystems C600 (Azure).

3.4 High-resolution respirometry

To obtain high-resolution respirometry data, I used O2k Oroboros Oxygraph instrument. This device measures changes of oxygen concentration in closed chamber over time. I followed standardized protocols to measure respiration of individual complexes using various substrates and inhibitors of respiratory chain (Kluckova et al., 2015; Pesta and Gnaiger, 2012; Rohlenova et al., 2017). Cells were collected by trypsine and resuspended in 2.5 ml of MIR05 medium (0.5mM EGTA, 3mM MgCl2, 60mM K Lactobionate, 20mM taurine, 10mM KH2PO4, 110mM sucrose, 1g/l BSA, 20mM HEPES, pH 7.1) in concentration 1 million of cells per 1 ml. After measurement of routine respiration, cells were permeabilized by digitonin (10µg/1million of cells) and specific respiration of single complexes was measured using particular substrates and inhibitors of respiratory chain. Specifically, glutamate and malate and succinate as substrates for Complex I and Complex II, respectively and ascorbate with TMPD as artificial substrates for Complex IV. To evaluate maximal potential of respiratory chain, respiration was measured in uncoupled state obtained by CCCP. Specific inhibitors of Complex I (rotenone), Complex II (malonate), Complex III (antimycin) and Complex IV (KCN) were used.

3.5 Lactate production assay

15 thousand cells were plated into 96-well plate 48 hours before experiment. 24 hours before experiment, medium was changed for 100 µl of fresh one. To measure lactate production, Lactate kit (TrinityBiotech, 735-10) was used following manufacturer's instructions with all volumes scaled down 10 times, in duplicates. Lactate standard (Trinity Biotech, 826-10) was used to quantify lactate production. As a blank, medium without cells was measured for lactate amount as well. Detection of lactate is based on changes of absorbance of Lactate reagent at 540 nm measured by TECAN instrument Infinite M200. Cells were further harvested in RIPA buffer and protein concentration measured by BCA Protein

Assay Kit (Thermo Fisher Scientific, 23225). Measured lactate production was corrected for protein amounts. Data were analysed by one-way ANOVA in GraphPad Prism software.

3.6 Flow cytometry

Flow cytometry measurements were performed using BD-Fortessa cell analyzer. All samples were measured in duplicates and analyzed in FlowJo software. Signal of 2-NBDG, DCF, MitoSOX and Annexin-V was measured using 488nm excitation laser and 560BP/40 detection filter for MitoSOX signal and 530BP/30 detection filter for other compounds. PI signal was measured using 561nm laser and 620BP/30 detection filter and Hoechst 33258 using 355nm laser and BP450/50 detection filter.

3.6.1 Glucose uptake

Fluorescently marked glucose, 2-(*N*-(7-Nitrobenz-2-oxa-1,3-diazol-4-yl)Amino)-2-Deoxyglucose, 2-NBDG (Life Technologies, N13195) was used to visualize glucose uptake. 200 thousand cells per well plated into 6-well plate 24 hours before experiment were incubated for 15 minutes in 50µM solution of 2-NBDG, trypsinized and resuspended in PBS. Uptake of 2-NBDG was measured by flow cytometry. Cell death was assessed by PI staining (5 ng/ml, P4864). Data were analysed by one-way ANOVA in GraphPad Prism software.

3.6.2 ROS production

200 thousand cells per well plated into 6-well plate 24 hours before experiment were incubated 15 minutes with 5µM DCFDA (2',7'-dichlorodihydrofluorescein diacetate, D6883) or 2,5 µM MitoSOX. Cells were collected with trypsin into PBS and stained by Hoechst 33258 (94403) to distinguish dead cells (final concentration 1 µg/ml). Geometric means of DCF signal were compared by one-way ANOVA in GraphPad Prism software.

DCFDA (2’,7’-dichlorofluorescin diacetate) is oxidized by reactive oxygen species in cell to DCF (dichlorofluorescein). The fluorescence generated is directly proportional to the amount of oxidized DCFDA to DCF. MitoSOX detects superoxides inside mitochondria of live cells. MitoSOX is selectively transported into mitochondria, where is oxidized and exhibits red fluorescence.

3.6.3 Cell Death Measurement

50 thousand cells per well were plated into 24 well plate 48 hours in advance. Optionally, cells were treated with 2μM MitoTam (synthetized in-house) 24 hours before collection. Dead cells from medium were collected by centrifugation and attached cells were collected with trypsin, centrifuged and resuspended in 1× Annexin Binding Buffer with 0.3 U/100 μl Annexin V-FITC (Apronex). After 5 minutes of incubation cells were stained with 1μg/ml Hoechst 33258 (94403). Cell death was calculated as summary pecentage of cells positive to only Annexin V, only Hoechst and positive to both staining. Data were analysed by one-way ANOVA in GraphPad Prism software.

3.7 Blue native gel electrophoresis

Five 150mm plates with cells (80% confluence) were scraped into cold PBS, centrifuged and resuspended in STE buffer (Vondrusova et al., 2015). Cells were homogenized in Balch homogenizer (Isobiotech) with insert allowing 8 μm slot. Homogenized cells were centrifuged (4°C, 5 min, 800 rcf), supernatant further centrifuged (4°C, 5 min, 3000 rcf) and eventually, mitochondria were collected by centrifugation (4°C, 15 min, 10 000 rcf). Pellet rich for mitochondria was resuspended in 100 μl of STE buffer.

Further on, the method was performed as in (Vondrusova et al., 2015). 8 g of digitonin (D141) per 1 g of protein was used to lyse mitochondria mildly. 25 μg of mitochondrial lysate was used per well in 3-12% polyacrylamide gel (Invitrogen, BN2011NX10) to run the native electrophoresis. After western blotting, membranes were incubated with primary antibody for NDUFA9 (Abcam, ab14713) and secondary antibody conjugated with HRP (Secondary anti-mouse antibody (Bio-Rad, 170-6516)). SuperSignal West Femto Maximum Sensitivity substrate (Thermo Fisher Scientific, 34096) was used for visualization of membranes recorded by CCD Azure Biosystems C600 (Azure).

50 μg of each sample was used to perform SDS-PAGE followed by western blotting and visualization of HSP60 protein as loading control.

3.8 Proliferation in 2D – crystal violet

5 thousand cells per well were plated into 96-well plate in 10 technical replicates. Cells were fixed after 24, 48, 72, and 96 hours in 4% paraformaldehyde for 30 minutes, washed in PBS and stained with 0.05% crystal violet (C3886) for 1h. Remaining crystal violet was washed

by PBS. Crystal violet bound to cells was dissolved into solution of 1% SDS and absorbance at 595 nm was measured using TECAN instrument Infinite M200. Data were analysed by two-way ANOVA in GraphPad Prism software.

3.9 Proliferation in 2D – IncuCyte

5 thousand cells per well were plated into 96-well plate (TPP) into DMEM medium. Cell proliferation was continuously monitored using an IncuCyte ZOOM Kinetic live cell imaging system (Essen BioScience, Ann Arbor, MI, USA) and measured as the phase object confluence percentage. All experiments were performed in triplicate and monitored for 6 days.

3.10 Scratch-wound healing assay

1.2 milion cells per well were plated into 12-well plate into DMEM medium with 1µg/ml Mitomycin C (M4287) one day before experiment. Confluent cells were scratched with yellow tip and incubated further in medium with Mitomycin C. Pictures were taken in starting time point (t0) using Leica DM IL LED Microscope, Leica DFC 450C Camera and LAS V4.5 software. A picture of the same part of the scratch was taken 8 hours later. An area without cell coverage was counted in FiJi software. Difference between areas was divided by time and related to parental cell line shown as relative speed of scratch-wound closure. Four windows per well were taken and averaged. Data were analysed by one-way ANOVA in GraphPad Prism software.

3.11 Growth in collagen

20 thousand cells were grown in 100 µl of collagen matrix (1x RPMI, 0.2% $NaHCO_3$, 447µM NaOH, 15mM HEPES, 50µM gentamicin, 1% FBS, 1mg/ml rat tail collagen) layered by phenol red free DMEM with 10% FBS (DMEM D5030, 4.5g/l glucose, 4mM glutamine, 1.8g/l $NaHCO_3$, 10% FBS (F7524), 100U/ml Penicillin (P3032) and 100µg/ml Streptomycin (S9137)). After 48 hours medium was replaced with 20% Alamar blue (Thermo Fisher Scientific, DAL1100) in DMEM and incubated with cells for next 4 hours. Alamar blue is reduced when absorbed by cells and changes its fluorescent properties. Gain of fluorescence is proportional to cell amount in collagen and it was measured by TECAN instrument Infinite M200 using excitation at 560 nm and emission measurement at 590 nm. As a blank, collagen without cells was used. Three technical replicates were used in every experiment and data were analysed by one-way ANOVA in GraphPad Prism software.

3.12 Migration in collagen

Cell lines were grown as spheroids (500 cells per spheroid) using 3D Petri Dish® (Microtissues®; #12-81 large spheroids) and 2% agarose in PBS according to manufacturer protocol for 3 days (DMEM with 10 % serum). Then, micro-moulds formed by 2% agarose with 81 micro-spheroids per well were overlaid by 190 µl collagen matrix similarly as in (Ravid-Hermesh et al., 2018); final concentration of rat tail collagen 1 mg/ml , 1% serum, 1× DMEM, 15mM HEPES, 477µM NaOH, 0.4% $NaHCO_3$ and 5µg/ml folic acid. Type I collagen was extracted from rat tail tendons via acid-solubilization, purified via centrifugation and precipitation, and dialysed in 0.1% acetic acid at 4 mg/ml. Invasion assay was performed in 12-well plates (81 micro-spheroids per well for each variant). Collagen matrix in each well was overlaid with the cultivation medium with 1% FBS. Images of spheroids were taken immediately after embedding of spheroids in collagen and then 24 hours after using Nikon Eclipse TE2000-S microscope (4x/0.13 PH1 and PHL objective). Cell invasion was calculated as the area of migrating cells after 24 hours after subtracting of the initial area value of spheroid using a macro in ImageJ. Statistical analyses were performed by the SigmaPlot software package (Systat Software, Inc.) using two-way ANOVA followed by Holm Sidak's post hoc comparison. Presented data are summarized from three independent experiments.

3.13 Colony forming assay in agarose

50 thousand cells were plated into 0.35% agarose (Nippon Genetics, AG02) in DMEM in 100mm Petri dish. Cells were cultivated for 3 weeks. Pictures of colonies growing in agarose were taken by AxioZoom.V16 Macrscope. Field of size 4,4×3,5cm was taken and number of colonies in this field bigger than 2000 μm^2 was counted in ImageJ software for each Petri dish. Number of colonies were compared by one-way ANOVA in GraphPad Prism software.

3.14 *In vivo* tumour growth

Female immunodeficient NSG-SGM3 mice were housed in the animal facility of the institute of Molecular Genetics, Czech Academy of Sciences. Mice were kept on normal diet and fed *ad libitum*. 6 mice per group were used. 0.7 million cells were injected subcutaneously in the right flank of each mouse using a gage 26 needle. Tumour growth was followed for 43 days using calliper measurements twice weekly. Mice were sacrificed at day 43, tumours were excised and weighted.

4 Results

4.1 Kinase mutants preparation

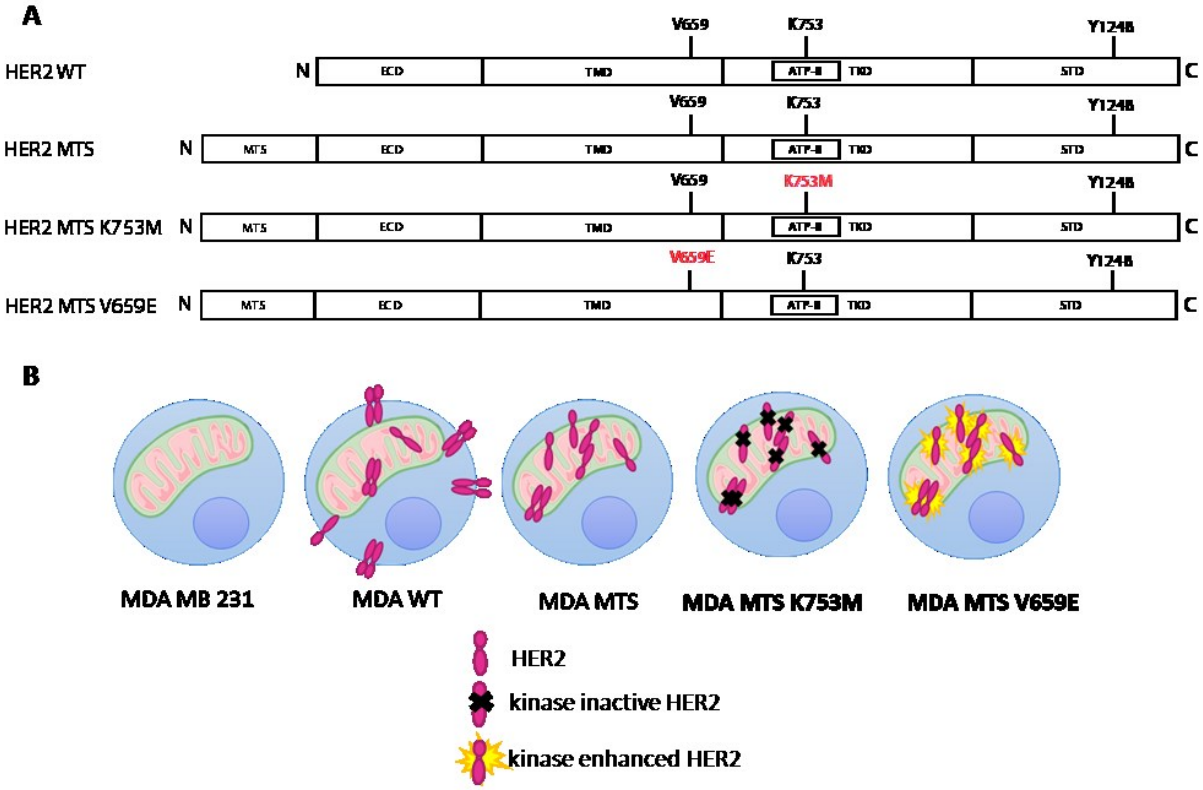

Figure 4.1: ***(A) Scheme of the HER2 variants:*** *MTS – mitochondria targeting sequence, ECD – extracellular domain, TMD – transmembrane domain, ATP-B – ATP-binding site, TKD – tyrosine kinase domain, STD – signal transducing domain.* ***(B) Visual interpretation of the experimental model***

I worked with experimental model based on MDA MB 231 cancer cell line. MDA MB 231 cell line is triple negative – it lacks estrogen receptor, progesterone receptor and the most importantly HER2 expression. Thus, overexpression of different HER2 constructs, which I describe further, is not influenced by endogenous HER2. Based on previous work in our laboratory, I could use already prepared cell lines overexpressing variants of HER2 – WT (overexpressing wild type HER2) and MTS (overexpressing HER2 targeted into mitochondria by N-terminal MTS of protein COX8) (Rohlenova et al., 2017).

To study kinase activity of mitochondrial HER2, I prepared kinase mutants of HER2-MTS using QuickChange site directed mutagenesis. Kinase deficient mutant HER2-MTS K753M, unable to bind ATP, and kinase-enhanced mutant, HER2-MTS V659E, were cloned into pEF/IRES/Puro vector and overexpressed in MDA MB 231 cells (Fig. 4.1).

After transfection, populations originating from single cell were collected and HER2 expression evaluated. To obtain a clone with a similar expression of mutated HER2 as in previously used lineages, I selected them based on western blotting analysis. For future experiments cl. 9 of MDA MTS K753M (kinase dead mutant) and cl. 8 of MDA MTS V659E (kinase active mutant) were used (Fig. 4.2).

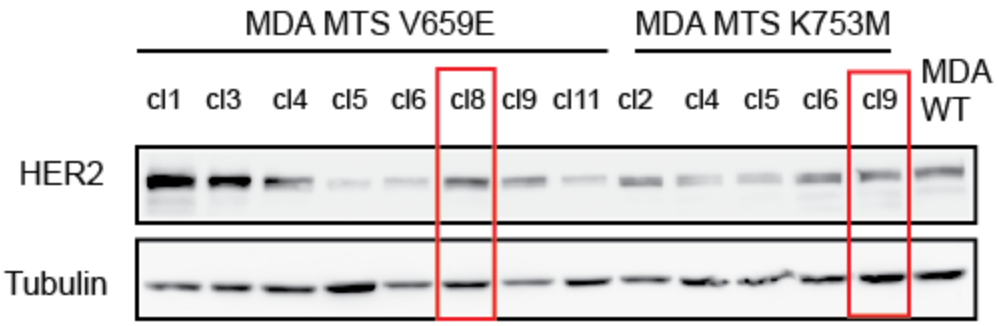

Figure 4.2: ***Western blot analysis of clones****: Clones originating from single cell were collected after transfection with expression plasmids. HER2 level was assessed by SDS-PAGE followed by western blotting. 50 µg of protein was used for each well, tubulin was used as loading control.*

4.2 HER2 role in mitochondria is distinct from canonical HER2 signalling.

AKT pathway is strongly involved in HER2 canonical signalling from the plasma membrane. Therefore, the role of mitochondrially targeted variants of HER2 in AKT signalling was evaluated (Fig. 4.3 A). Expectedly, overexpression of WT-HER2 led to an activation of AKT pathway visualized as its phosphorylation on Ser473. However, mitochondrial HER2 did not drive Ser473 phosphorylation. Hence, IMM localization does not stimulate HER2 canonical signalling.

Previously, it was shown that at elevated H_2O_2 concentration, AKT translocates into mitochondria and participates in further induction of ROS production and apoptosis (Antico Arciuch et al., 2009; Iskandar et al., 2016). Thus, AKT content in mitochondria was investigated in cells with HER2 variants (Fig. 4.3 B). There were no differences in AKT localization into mitochondria observed among cell lines, though.

From these experiments it was concluded that the mechanism of HER2 action in mitochondria does not include AKT activation.

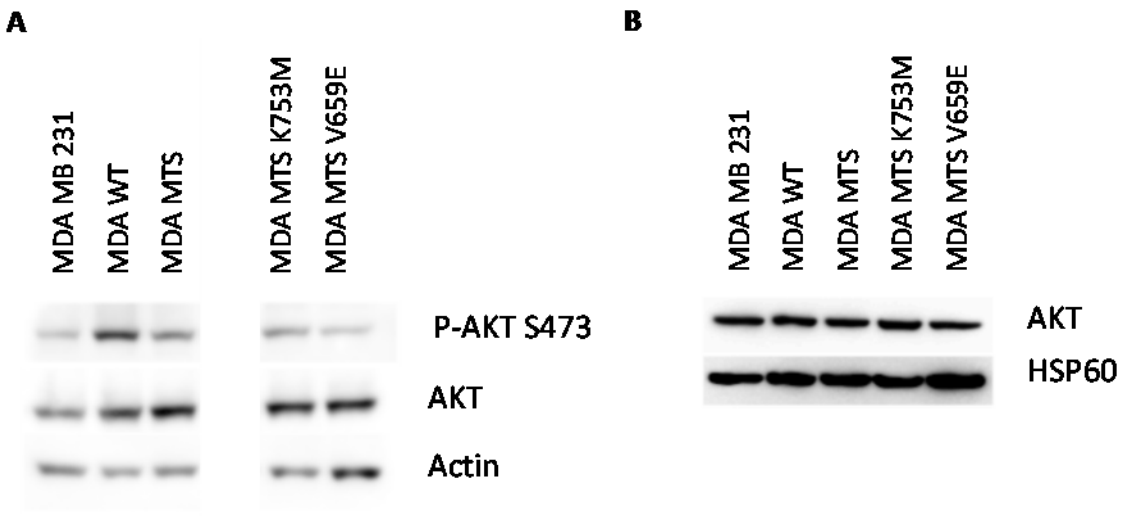

Figure 4.3 ***AKT activation: (A)*** *Whole cell lysates were analysed by SDS-PAGE followed by western blotting. Antibodies against phosphorylated AKT and total AKT were used. 50 µg of protein was used for each well, tubulin was used as loading control. All samples were on the same gel and membrane, irrelevant sample was subtracted.* ***(B)*** *Crude mitochondrial lysates were analysed by SDS-PAGE followed by western blotting. Localization of AKT to mitochondria was assessed. HSP60 was used as a loading control.*

4.3 Kinase activity of mitochondrial HER2 accelerates metabolism

Here I would like to uncover the contribution of main metabolic pathways – glycolysis and OXPHOS in cells with variants of HER2. Elevated respiration of MCF7 cells overexpressing HER2 was shown previously (Rohlenova et al., 2017). Even though HER2-WT did not drive any significant changes in respiration of MDA MB 231 cells, higher respiration was dependent on tyrosine kinase activity of mitochondrial HER2. The respiration rate of MDA MTS V659E cells reached MDA MTS values in case of Complex I, Complex II and Complex IV, too. On the other hand, respiration of kinase deficient mutant (MDA MTS K753M) was similar to the level of parental cells (Fig. 4.4 A).

Glucose uptake grew with kinase activity of HER2-MTS. Constitutive kinase activity (in MDA MTS V659E cells) demanded around 50% increase in glucose uptake (Fig. 4.4 B). The elevated glucose utilization dependent on kinase activity of mitochondrial HER2 was supported by increased lactate production observed (Fig. 4.4 C).

I found elevated respiration, while glycolysis is not significantly affected in MDA MTS cells. However, constitutive kinase activity of mitochondrial HER2 drives both respiration and glycolysis leading to overall faster metabolism.

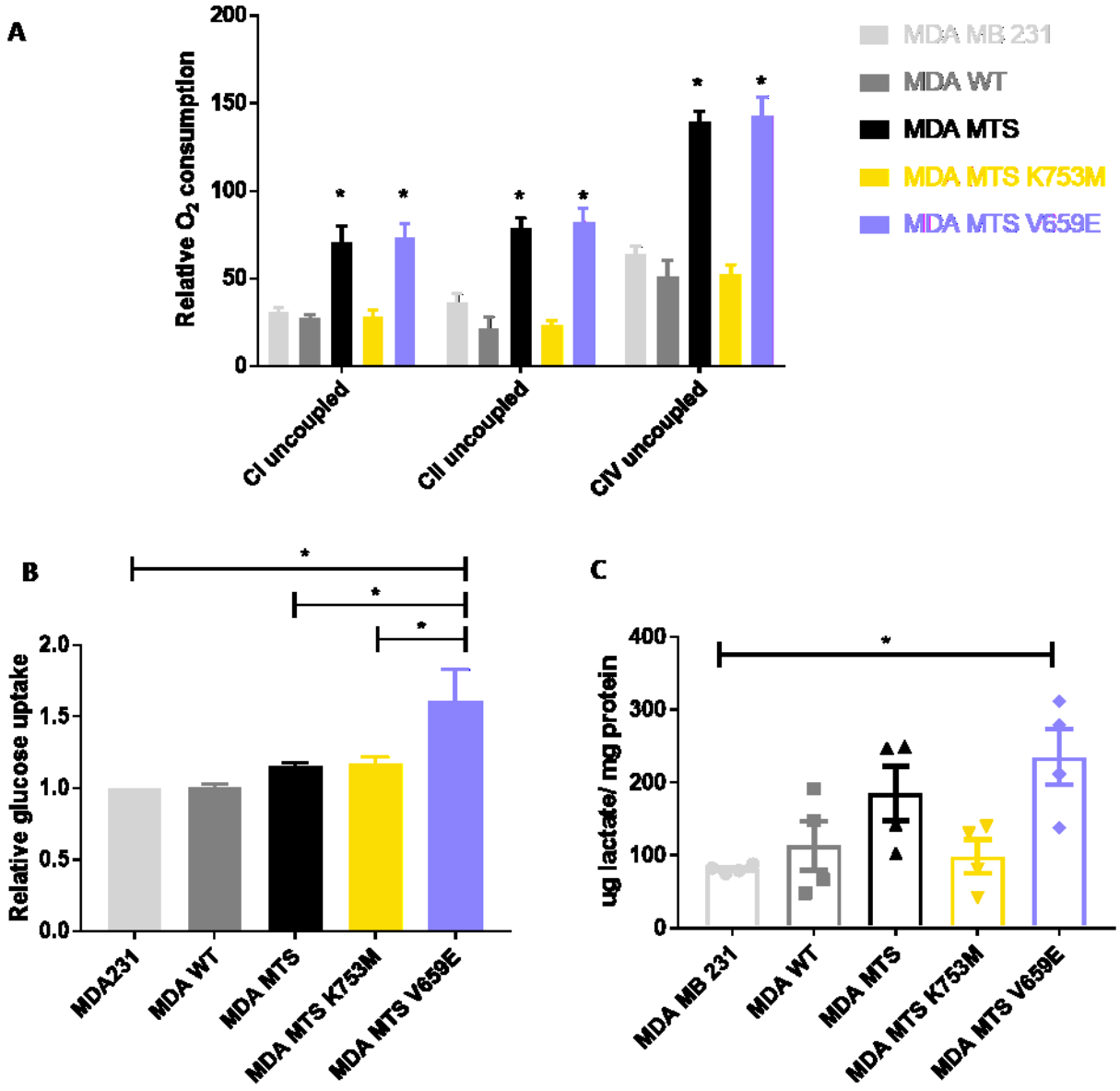

Figure 4.4: ***(A) High-resolution respirometry****: Relative O2 consumption of permeabilized cells is depicted in pmol[O2]/(s*mil) where „mil" is number of cells in milion. Specific respiration of individual respiratory complexes is shown. Statistical analysis: ordinary two-way ANOVA followed by Tukey's multiple comparisons test, n=4, SEM is shown, significance of comparison to MDA MB 231 is marked with asterisks (p<0.001).* ***(B) Glucose uptake:*** *Relative glucose uptake stands for geometrical mean of 2-NBDG fluorescence signal relative to MDA MB 231. Statistical analysis: ordinary one-way ANOVA followed by Tukey's multiple comparisons test, with a single pooled variance, n=5, SEM is shown, significant changes marked with asterisks (p<0.05).* ***(C) Lactate production:*** *Amount in µg of lactate produced by cells into medium in 24h relative to mg of protein and corrected to background signal is depicted. Statistical analysis: ordinary one-way ANOVA followed by Tukey's multiple comparisons test, with a single pooled variance, n=4, SEM is shown, significant changes marked with asterisk (p<0.05).*

4.4 Tyrosine kinase active mutant of mitochondrial HER2 displays elevated cell death correlating with increased ROS production and low assembly of supercomplexes

MDA MTS V659E exhibit a strong phenotype, thus I noticed elevated cell death of these cells. To confirm this observation, viability of cells with variants of HER2 was measured. Constitutive tyrosine kinase activity of mitochondrial HER2 increases basal level of cell death. Neither MDA MTS K753M nor MDA MTS share this characteristic (Fig. 4.5 A).

MitoTam is a potential anti-cancer agent affecting mitochondrial respiratory chain. Previously, it was shown that its effect significantly rises with HER2 overexpression and localization into mitochondria in MCF7 cell line (Rohlenova et al., 2017). Cells with HER2 variants were treated for 24h with 2μM MitoTam and cell death was assessed. Only mild increase in susceptibility to MitoTam of MDA MB 231 with HER2-WT and HER2-MTS overexpression was observed. However, I observed twice higher effect of MitoTam in kinase enhanced mutant than in the kinase dead counterparts (Fig. 4.5 B). This suggests that kinase activity of mitochondrial HER2 drives susceptibility to MitoTam.

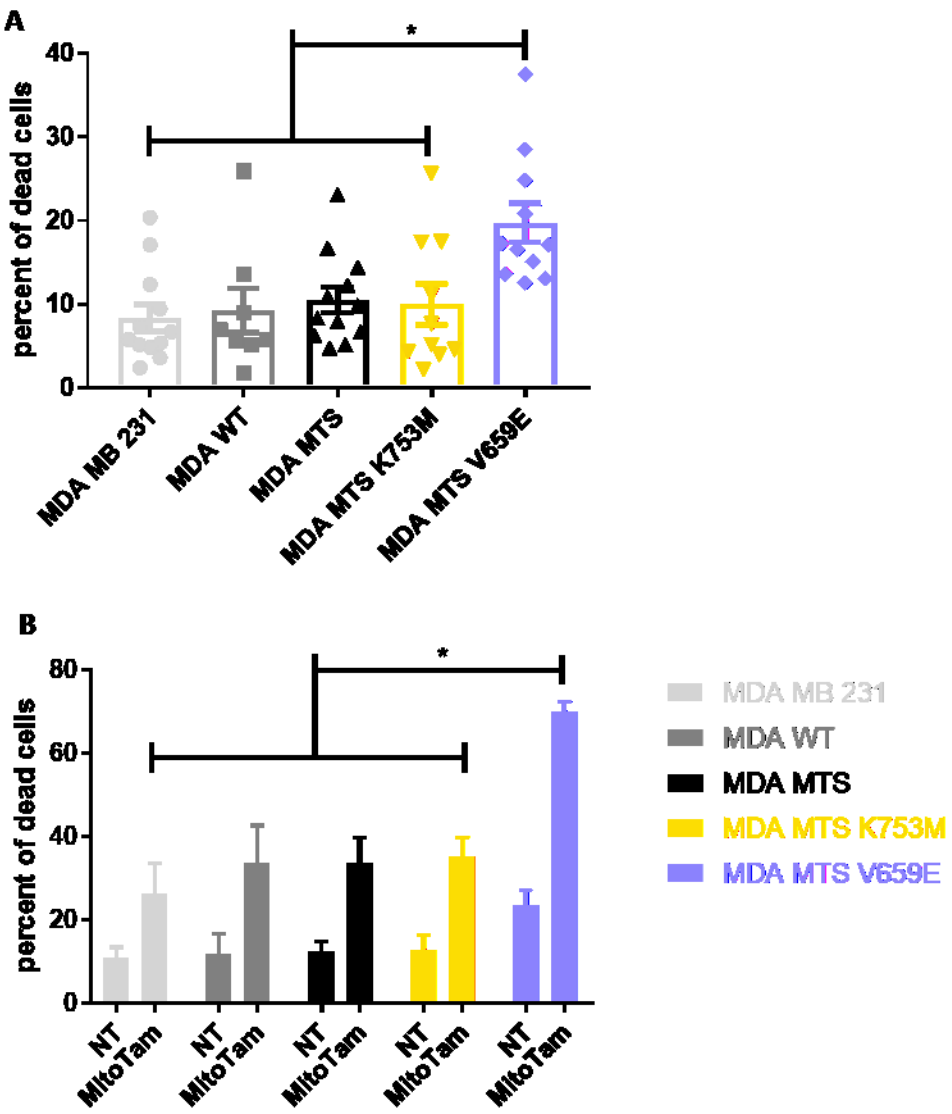

Figure 4.5: ***(A) Cell death measurement:*** *Cell death was measured after staining with Annexin V and Hoechst 33258 by flow cytometry. Statistical analysis: ordinary one-way ANOVA followed by Tukey's multiple comparisons test, with a single pooled variance, n=8 for MDA WT, n=12 for remaining cell lines, SEM is shown, significant changes marked with asterisks, p<0.05.* ***(B) MitoTam sensitivity****: Cells were treated with 2μM MitoTam for 24h and cell death was measured after staining with Annexin V and Hoechst 33258 by flow cytometry. Statistical analysis: ordinary two-way ANOVA followed by Sidak's multiple comparisons test, n=4 for MDA WT, n=6 for remaining cell lines, SEM is shown, significant changes marked with asterisks, p<0.001.*

The proposed mechanism of MitoTam function is interaction with respiratory complexes and induction of ROS production. Oxidative stress leads further to cell death. Thus, elevated basal cell death and high susceptibility to MitoTam treatment of MDA MTS V659E cells might be caused by higher basal level of ROS. DCF staining for visualization of cellular ROS was performed. Higher baseline ROS production was observed in cells overexpressing mitochondrially targeted HER2, and was dependent on its tyrosine kinase activity (Fig. 4.6 A).

However, the level of ROS in MDA MTS and MDA MTS V659E was similar. It did not explain higher cell death in MDA MTS V659E cells. Thus, cells were probed with MitoSOX – an agent that detects mitochondrial ROS specifically. This experiment displayed elevated mitochondrial ROS in MDA MTS V659E compared to all other cell lines (Fig. 4.6 B). In conclusion, increased cell death of MDA MTS V659E cells is associated with a high basal level of mitochondrial ROS production.

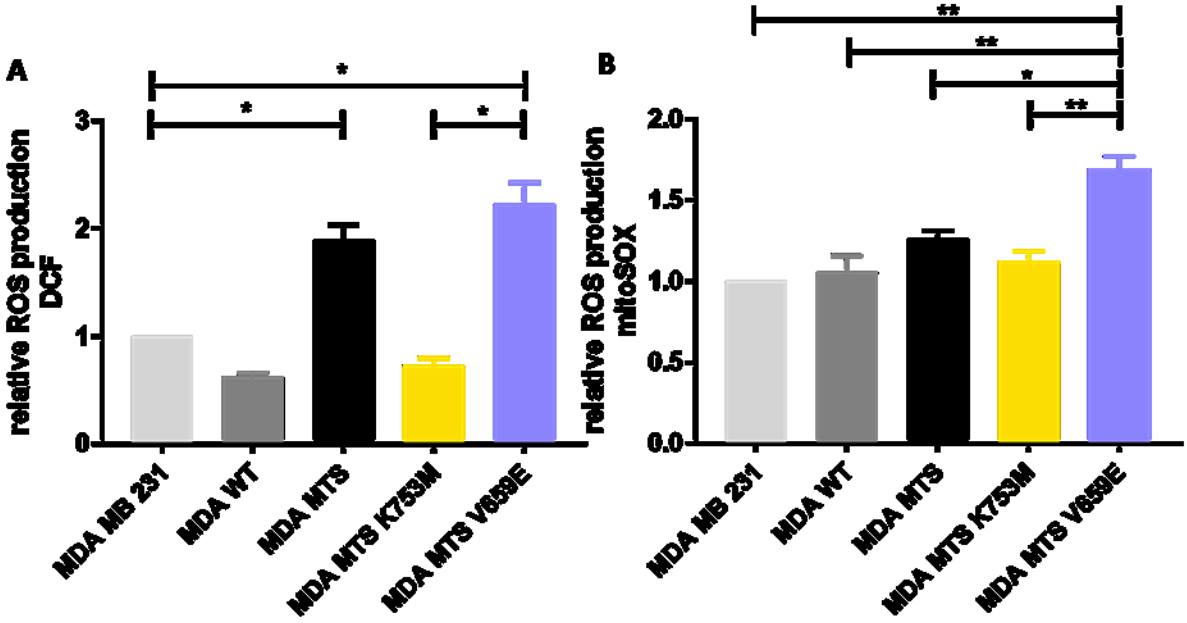

Figure 4.6: ***ROS production****: **(A)** Fluorescent signal of DCF probe was measured by flow cytometry. Geometric mean of DCF signal related to MDA MB 231 is shown. Statistical analysis: ordinary one-way ANOVA followed by Tukey's multiple comparisons test, with a single pooled variance, n=11 in MDA MB 231, MDA MTS and MDA MTS V659E, n=9 in MDA WT and MDA MTS K753M, SEM is shown, significant changes marked with asterisks, p<0.0001.* ***(B)*** *Fluorescent signal of MitoSOX probe was measured by flow cytometry. Geometric mean of MitoSOX signal related to MDA MB 231 is shown. Statistical analysis: ordinary one-way ANOVA followed by Tukey's multiple comparisons test, with a single pooled variance, n=5, SEM is shown, significant changes marked with asterisks, * p<0.01, ** p<0.0001.*

In (Rohlenova et al., 2017) blocking of HER2 transport into mitochondria led to lowered assembly of supercomplexes. Thus, it was suggested that mitochondrial pool of HER2 facilitates supercomplex formation. I performed Blue Native Gel Electrophoresis to visualize respirasomes using antibody against a subunit of Complex I (NDUFA 9). Higher assembly of respiratory supercomplexes in MDA MTS tightly correlates with its elevated respiratory rates. In contrast, constitutive kinase activity of mitochondrial HER2 disrupts supercomplexes formation. While kinase dead mutant (MDA MTS K753M) keeps highly assembled supercomplexes, kinase active mutant (MDA MTS V659E) loses this feature (Fig. 4.7). These finding was rather surprising as respiration is unaffected in MDA MTS V659E compared to MDA MTS. However, it correlates with enhanced glycolysis in these cells and elevated basal production of ROS in mitochondria.

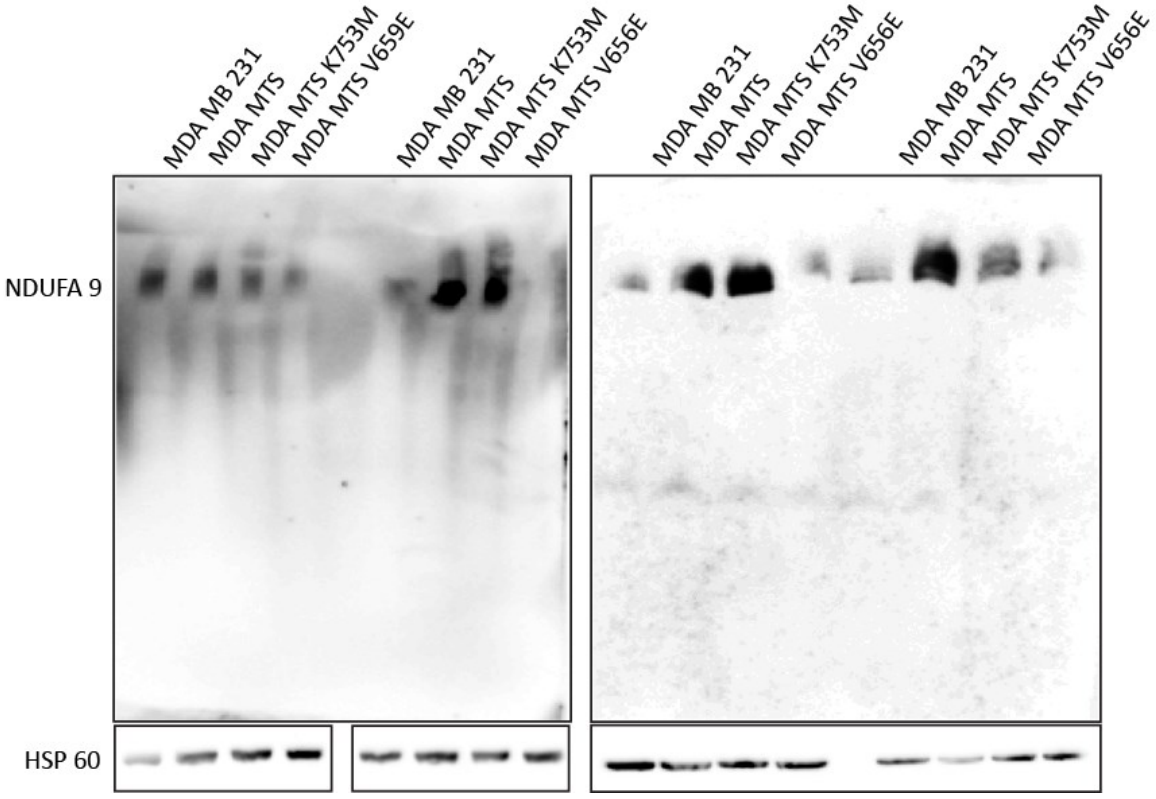

Figure 4.7: ***Blue native gel electrophoresis****: 25 µg of protein isolated from mitochondrial fraction was probed for respirasome by western blotting following blue native gel electrophoresis in 4 biological replicates. HSP60 visualized by western blotting after SDS-PAGE was used as a loading control.*

4.5 Constitutive kinase activity of mitochondrial HER2 enhances *in vitro* proliferation and migration but impairs tumour growth *in vivo*

The first main feature of cancer cell is the ability to proliferate. To evaluate tumorigenicity, I examined proliferation rates in common cultivation dish, in 3D condition and *in vivo.* For cancer development and metastatic cascade progression cells need to gain high motility. Thus, migration assays were also performed.

I evaluated proliferation in 2D by crystal violet staining (Fig. 4.8 A). After 72h incubation, MDA MTS cells produced approximately twice more cell mass than parental cell line. Similarly, kinase enhanced mutant (MDA MTS V659E) featured increased cell growth, while proliferation rate of MDA MTS K753M was similar to cell lines lacking mitochondrial HER2. This suggests that elevated proliferation of MDA MTS in these conditions is dependent on its kinase activity. Data obtained by crystal violet staining were confirmed using IncuCyte instrument, where proliferation is measured in real time (Fig. 4.8 B).

The migration in 2D conditions was measured in scratch-wound healing assay. Confluent layer of cells was scratched by a tip removing part of the layer (wound). Cells migrated into the wound in following 8 hours with different speed. To prevent wound closure due to enhanced cell proliferation, cells were treated with Mitomycin C which crosslinks DNA and arrests cell cycle. Thus, it is assumed that any differences observed in this assay reflect only changes in cell motility, not proliferation. My results indicate that MDA MTS cells migrate about 2.7 times faster than cells without mitochondrial HER2. Average speed of migration of kinase mutants clearly show that this feature is dependent on HER2 tyrosine kinase activity as MDA MTS V659E cells reach MDA MTS velocity, while MDA MTS K753M motility was similar to the cells without mitochondrial HER2. (Fig. 4.8 C).

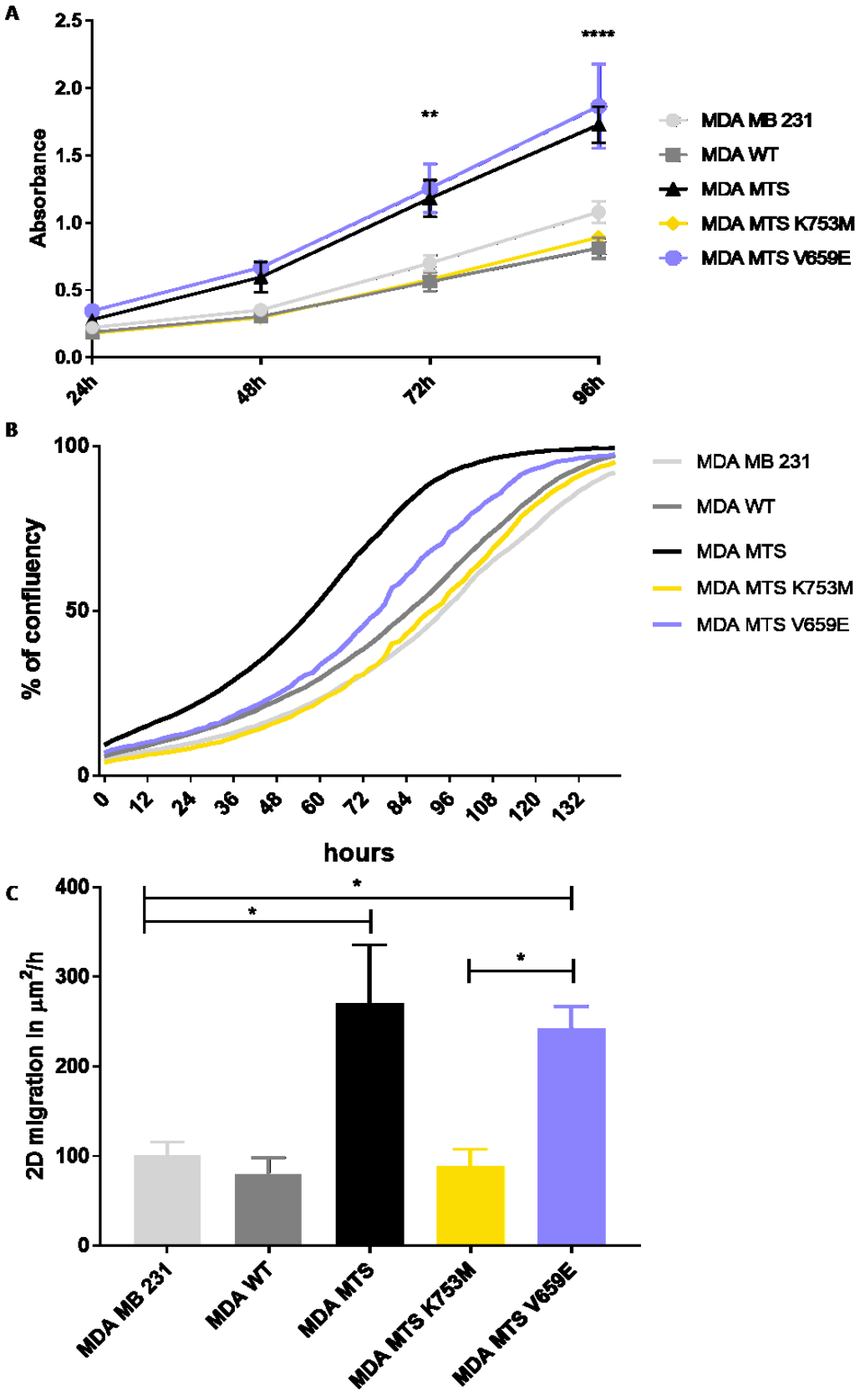
A
Absorbance
2.5
2.0
1.5
1.0
0.5
0.0
24h
48h
72h
96h
**
****
MDA MB 231
MDA WT
MDA MTS
MDA MTS K753M
MDA MTS V659E
B
% of confluency
100
50
0
0
12
24
36
48
60
72
84
96
108
120
132
hours
MDA MB 231
MDA WT
MDA MTS
MDA MTS K753M
MDA MTS V659E
C
2D migration in µm²/h
400
300
200
100
0
*
*
*
MDA MB 231
MDA WT
MDA MTS
MDA MTS K753M
MDA MTS V659E

Figure 4.8: ***Tumorigenic potential in 2D conditions: Proliferation: (A)*** *Absorbance of crystal violet staining measured at 595 nm displays cell growth in time. Statistical analysis: ordinary two-way ANOVA followed by Dunett's multiple comparisons test, n=4, SEM is shown, significant changes between MDA MB 231 and MDA MTS and MDA V659E marked with asterisk: ** p<0.01, **** p<0.0001.* ***(B)*** *Cell growth was measured using IncuCyte instrument. Percentage of confluence was analysed every 2 hours for 6 days. Three independent experiments were taken, representative one is shown. Every curve is an average of three technical replicates.* ***(C) Scratch-wound healing assay:*** *Migration speed in μm²/h shows average difference of scratch area among time points. Statistical analysis: ordinary one-way ANOVA followed by Tukey's multiple comparisons test, with a single pooled variance, n=4, SEM is shown, significant changes marked with asterisk, p<0.05.*

Nevertheless, cultivation plastic may not be representative of *in vivo* conditions. Thus, I used 3D matrices allowing growth with attachment to extracellular matrix (collagen) and without attachment (agarose) to imitate *in vivo* situation better. Similarly to 2D, growth in 3D collagen was enhanced in cells with mitochondrial HER2 with kinase activity unchanged or constitutively active. MDA MTS K753M cells exhibited similar growth rate as cells without mitochondrial HER2 enrichment (Fig. 4.9 A). In collaboration with Jakub Gemperle in the laboratory of doc. Brábek and doc. Rösel, 3D migration assay was performed. Cells were grown in agarose wells allowing them to form spheroids. These spheroids were further embedded into collagen and migration from the spheroids through collagen was observed. The area in which migrating cells were observed is shown in figure 4.9 B. Cells with mitochondrial HER2 migrate more than parental cells or cells with WT-HER2. However, this effect was independent on kinase activity of HER2-MTS, as even kinase dead mutant increased cell migration.

Even though kinase activity of mitochondrial HER2 seemed to drive tumorigenicity of breast cancer cells based in 2D experiments, next investigation brought surprising findings. Studied cell lines were plated into 0.35% agarose. In this condition, cells grow without attachment which better mimic obstacles cancer cells have to overcome during *in vivo* tumorigenesis. After 3 weeks of growth in agarose, a number of colony forming units was assessed. HER2 overexpression did not provide any advantage in this assay. Even though MDA MTS cells were able to grow in agarose to some extent, their kinase enhanced mutant (MDA MTS V659E) lacked the ability to grow adherence-independently unlike MDA MTS K753M. In sharp contrast with the behaviour during adherent growth, constitutive kinase activity of mitochondrially targeted HER2 supressed growth in non-adherent conditions (Fig. 4.9 C).

As growth and migration of cells varies among several environments tested, we decided for *in vivo* experiment to assess the tumorigenic potential of cells with variants of HER2-MTS. Immunocompromised NSG-SGM3 mice were injected subcutaneously, tumour growth was followed in time, and tumour weight was evaluated after 43 days. Unexpectedly, cells with kinase active mutant, MDA MTS V659E, displayed inhibited growth of primary tumour *in vivo* compared to their kinase dead or unaltered counterparts (Fig. 4.9 D).

In conclusion, it appears that the effect of HER2-MTS is dependent on the cultivation conditions. Cells with kinase active HER2-MTS are unable to grow without attachment, which probably impairs subcutaneous tumour growth. Furthermore, the changes in tumorigenicity and metabolism observed in cells with mitochondrial HER2 might be driven by higher ROS production. Levels of mitochondrial ROS in MDA MTS V659E cells could cause disability to grow in unfavourable conditions such as in agarose (growth without attachment) and *in vivo*.

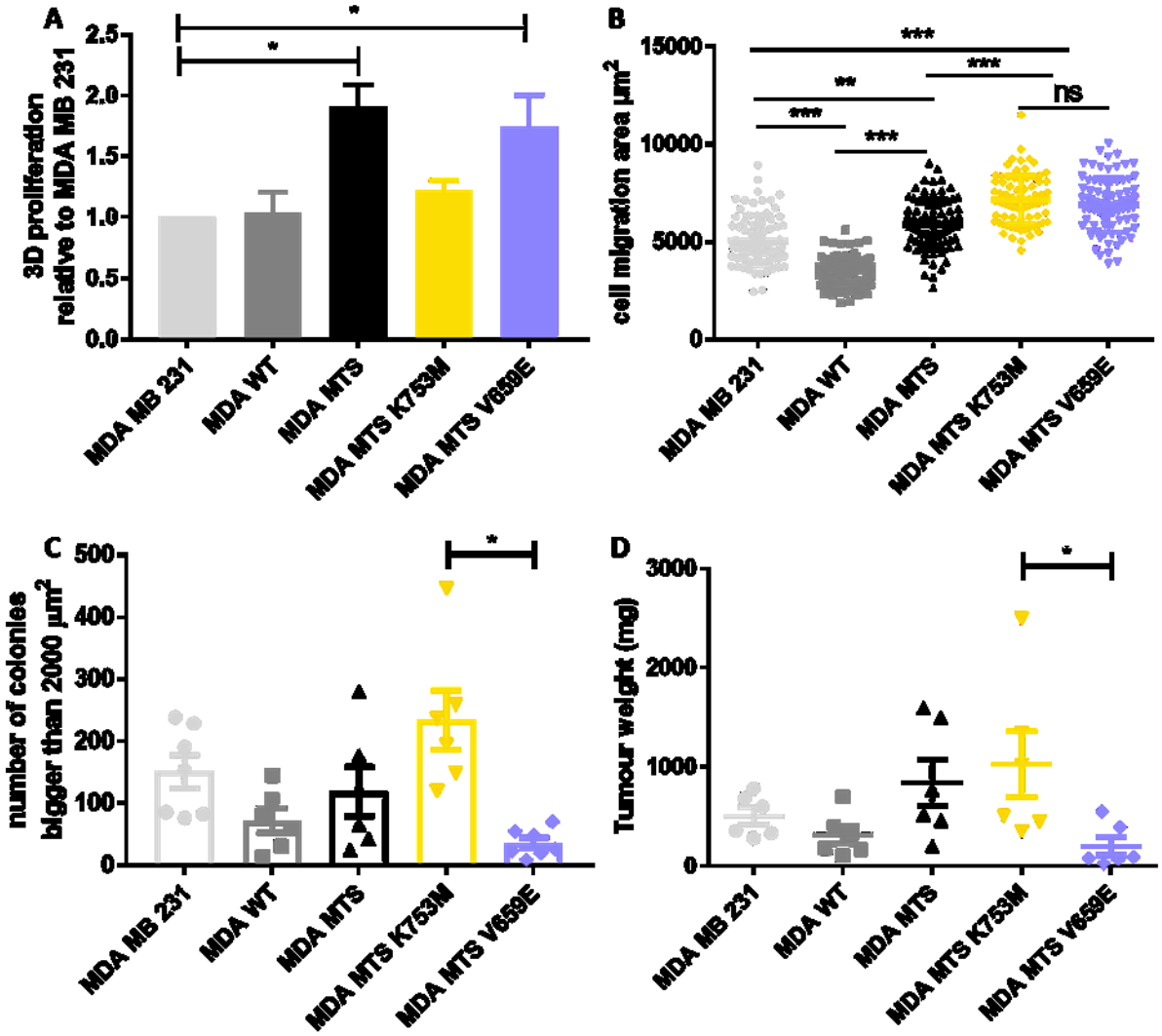

Figure 4.9: ***(A) Proliferation in collagen:*** *Cells were grown in collagen for 48 hours and further incubated with Alamar blue staining for next 4 hours. Reduction of Alamar blue was proportional to cell number and measured as fluorescence. Background fluorescence was substracted and data relativized to parental cell line. Statistical analysis: ordinary one-way ANOVA followed by Tukey's multiple comparisons test, with a single pooled variance, n=4, SEM is shown, significant changes marked with asterisks, p<0.05* ***(B) Migration in collagen****: Cell migration area normalized to spheroid size 24h after embedding into collagen matrix. Statistical analysis: two-way ANOVA followed by Holm Sidak's post hoc comparison. Presented data are summarized from three independent experiments, 20 spheroids were evaluated in each. Significant changes are marked with asterisks, ** p<0.01, *** p<0.001.* ***(C) Growth in agarose:*** *Number of colonies bigger than 2000 µm² grown for 3 weeks in 0.35% agarose were counted in ImajeJ software. Statistical analysis: ordinary one-way ANOVA followed by Tukey's multiple comparisons test, with a single pooled variance, n=7 for MDA MB 231 and MDA MTS V659E, n=6 for remaining cell lines, SEM is shown, significant changes marked with asterisks, p<0.001.* ***(D) in vivo growth:*** *The graph shows tumor weight after 43 days post injection of 6 NSG-SGM3 mice per group. Statistical analysis: ordinary one-way ANOVA followed by Tukey's multiple comparisons test, with a single pooled variance, n=6, SEM is shown, significant changes marked with asterisks, p<0.05.*

5 Discussion

HER2^{high} breast cancer is a frequent malignant disease with a poor prognosis for patients (Slamon et al., 1987). Thus, HER2 oncogene has been extensively studied in the past few decades – to date, PubMed database counts almost 29 thousand articles containing ERBB2 entry. Even though several approaches to HER2^{high} breast cancer therapy have been established, many patients develop resistance to treatment leading to relapse (Hynes and Lane, 2005). Anti-HER2 agent trastuzumab (Herceptin) is effective only in one third of patients in a long term (Vogel et al., 2002). One of the proposed mechanism of HER2^{high} breast cancer resistance to common treatment targeting HER2 might be HER2 localization into mitochondria (Ding et al., 2012). It hides inside mitochondria from therapeutic agent, where it further maintains malignant phenotype of cancer cells. Confirmation of this finding would considerably impact the mitochondrial HER2 studies.

HER2 oncogene hidden in an inner mitochondrial membrane affects essential bioenergetic pathways (Ding et al., 2012; Rohlenova et al., 2017). In its primary site, the plasma membrane, HER2 activates downstream targets through tyrosine kinase activity. Kinase activity of mitochondrial HER2 seems to be preserved – localization of HER2-WT is dependent on its kinase activity and HER2 translocation into mitochondria was shown in several tissues and cell lines (Ding et al., 2012).

Here I constructed tyrosine kinase mutants to evaluate the role of kinase activity of HER2 in mitochondria. Impairing kinase function of mitochondrial HER2 in MDA MTS K753M cells by ATP-binding site alteration often brought phenotype similar to cells without HER2 or overexpressing HER2-WT. From behaviour of cells with constitutively kinase active mitochondrial HER2, MDA MTS V659E, it is clear that kinase activity of HER2 is relevant in mitochondria.

AKT pathway is activated abundantly by plasma membrane HER2 overexpression (Antico Arciuch et al., 2009; Ram and Ethier, 1996). However, activation of canonical AKT pathway by mitochondrially targeted HER2 was not observed in this work. Neither activation by phosphorylation, nor translocation of AKT into mitochondria was identified. Thus, I conclude that the mechanism of action of mitochondrial HER2 is distinct from plasma membrane HER2 signalling.

An obvious but challenging question arises: What is the target of mitochondrial HER2 tyrosine kinase activity? Ding et al. (2012) suggested association of mitochondrial HER2 with cytochrome c oxidase subunit, while possible association with Complex I of respiratory chain comes from HER2^{high} cells being sensitive to MitoTam (Rohlenova et al., 2017). Phosphoproteomics analysis of kinase mutants, done in the laboratory, revealed possible direct phosphorylation targets with NDUFA13 (GRIM19), a subunit of Complex I, being the most promising (data not shown). Despite an intensive effort to reveal the molecular mechanism of HER2 function in mitochondria, this connection has not yet been confirmed.

It is reasonable to focus mitochondrial HER2 studies on its role in energy metabolism, as mitochondria stand in its centre. Ding et al. (2012) showed enhanced glucose uptake and lactate production in MDA MB 231 cells overexpressing mitochondrial HER2, but not in kinase deficient mutant. Even though I could not prove significant increase of glucose uptake in MDA MTS cells, lactate production was elevated. Kinase enhanced variant featured both elevated glucose utilization and higher lactate production suggesting a stronger involvement of glycolysis pathway than in other cell lines.

Ding and colleagues (2012) observed lower respiration of MDA MTS cells. Considering enhanced glucose utilization in this cell line, they proposed that mitochondrial HER2 switches metabolism of cancer cells from respiration to glycolysis. However, it is difficult to follow their experimental setup as they use mostly commercial assay kits, their methodology is not always transparent and notably varies from approaches in my work. My results are in strong opposition. Cells overexpressing mitochondrially targeted HER2 exhibited high respiration rates dependent on its kinase activity. This view is supported by unpublished data from our laboratory showing HER2-MTS driven increase of respiration also in MCF7 cell line (data not shown). Furthermore, cells with HER2-MTS contain more assembled supercomplexes than cells without HER2 or with HER2-WT, which often correlates with increased rate of respiration (Lapuente-Brun et al., 2013). In concordance with presented data, assembly of supercomplexes was impaired after prevention of HER2 transport into mitochondria in MCF7 cells (Rohlenova et al., 2017). However, elevated respiration in cells with constitutively active mitochondrial HER2 (MDA MTS V659E) can't be explained by supercomplexes assembly.

Behaviour of MDA MTS V659E cells could be explained through elevated ROS production, though. Enhanced OXPHOS followed by elevated ROS levels was observed in leukemic cells previously (Khan et al., 2016). Cells with kinase active mitochondrial HER2 (MDA MTS and MDA MTS V659E) exhibited elevated cellular ROS and mitochondrial ROS were highest in MDA MTS V659E. Moreover, elevated ROS level drives glucose uptake (Liemburg-Apers et al., 2015) which nicely correlates with presented glucose uptake measurements. At this time we have to be content with a correlation as the causality remains elusive. The mechanism can be viewed from the other side, too. Enhanced glycolysis leads to increased TCA cycle flux generating reduced coenzymes feeding respiratory chain. Elevated NADH/NAD+ and FADH2/FAD ratios push complexes I and III of respiratory chain to produce ROS (Liemburg-Apers et al., 2015). This also tightly correlates with assembly of supercomplexes: higher assembly of respirasomes in MDA MTS cells protects them from superoxide formation and thus, mitochondrial ROS are low. On the other hand, even though MDA MTS V659E cells keep high respiratory rates, their respirasomes are weakly assembled and enhanced reduction of ETC manifests by elevated level of mitochondrial ROS. Considering this hypothesis right, elevated cellular ROS in MDA MTS measured by DCF staining remain unexplained and must be associated with other cellular features, such as reduced antioxidant defence that we did not examine.

Originating in Warburg's legacy, cancer cells were considered highly glycolytic. However, it has been shown that OXPHOS plays crucial role in cancer progression (Bajzikova et al., 2019; Sonveaux et al., 2008). Upregulation of glucose transporters expression was observed in differentiating muscle cells where higher glucose uptake supported enhanced function of respiratory chain (Mitsumoto and Klip, 1992; Remels et al., 2010). It can't be excluded that cancer cells with mitochondrial HER2 use similar strategy regulated by ROS level (Liemburg-Apers et al., 2015).

Elevated ROS synthesis stimulates pro-tumorigenic signalling, but excess ROS drives tumour cells to apoptosis (Moloney and Cotter, 2018). At the first sight, tyrosine kinase activity of mitochondrial HER2 and subsequent ROS formation seemed to be an advantage for cancer cell, and MDA MTS V659E cell line mimicked MDA MTS in some of the experiments. However, excess ROS caused by constitutive kinase activity of HER2-MTS diminished viability of MDA MTS V659E cells. Compared with MDA MTS, it can be

concluded that the cells are driven to apoptosis due to elevated level of mitochondrial ROS, while excess cellular ROS do not impair cell viability. I have already mentioned MCF7 model used for HER2 studies in our laboratory. We could not perform the all experiments in this cell line, as MCF7 MTS V659E cells were not viable. In spite of several attempts, this cell line was not established and data is not available. Most probably, this failure confirms decreased viability of cells carrying tyrosine active mitochondrial HER2, possibly due to increased mitochondrial ROS. Furthermore, MDA MTS V659E alternative is missing in cell line collection of Ding et al. (2012), even though they used this mutation in MDA MB 453 cell line. I can only speculate whether this was due to low cell viability of MDA MB 231 cells with HER2-MTS V659E overexpression.

MDA MTS V659E cells were more susceptible to MitoTam treatment compared to all other studied cell lines. MitoTam interacts with Complex I of respiratory chain and induces ROS production followed by cell death. It was already shown that MitoTam is efficient in killing $HER2^{high}$ breast cancer cells and even more successful in case of cells with mitochondrial HER2 overexpression (Rohlenova et al., 2017). It is not surprising that MDA MTS V659E cells, which maintain high basal level of ROS and display decreased viability even without treatment, were more sensitive to MitoTam than other studied cell lines. From this experiment it can be concluded that sensitivity to MitoTam increases with tyrosine kinase activity of mitochondrial HER2 fraction. Ding et al. (2012) have shown mitochondrial HER2 as a cause of resistance to anti-HER2 treatment and Rohlenova with colleagues (2017) introduced MitoTam, an anticancer agent highly efficient in cancer cells with tyrosine active mitochondrial HER2, which is now in a clinical trial. Hopefully, these studies will help to establish more precise diagnostics and improve personalized medicine, providing an alternative for $HER2^{high}$ tumours resistant to conventional HER2-directed treatments.

In the last chapter I focused on evaluating tumorigenicity of cell lines overexpressing HER2 variants through measuring their proliferation and migration in several conditions. Although *in vitro* experiments describe only limited aspects of cancer cell behaviour, they allow for a more precise control of experimental variables and better quantitative analysis. Nevertheless, given the reduced physiological relevance of *in vitro* models, growth of tumours originating from studied cell lines was assessed also in an animal model. *In vivo* experiment

highlights the need for complex approaches to this research question, as not all the observations *in vitro* and *in vivo* fully matched.

2D-cultures benefit from cheap and easy handling, high performance and reproducibility of such experiments (Kapałczyńska et al., 2018). Cell-to-cell and cell-to-ECM contacts are deformed and do not reflect *in vivo* situation, though. Cells in 2D cultures lose their native morphology (von der Mark et al., 1977) which leads to changes in signalling, differentiation and homeostasis (Kilian et al., 2010; Nelson and Bissell, 2006). Moreover, cells in 2D cultures have unlimited access to oxygen, nutrients and signal molecules in medium, while 3D and *in vivo* condition bring heterogeneity in nutrient supply (Kapałczyńska et al., 2018).

The first 3D culture was set more than 40 years ago growing primary culture in soft agar (Hamburger and Salmon, 1977). Since then many models have been established containing various scaffolds, co-cultures, and micro-fluidic environment mimicking body fluid flow (Katt et al., 2016). Sophisticated bioreactors allowing maintenance of many variables under strict control created new dimension for tissue engineering and 3D cultures are even close to commercial use in food industry (Mehta et al., 2019). Despite being relatively simple, 3D assays in my work bridge the gap between common cell culture and *in vivo* model.

Cell lines with HER2 variants were grown in collagen, a natural segment of extracellular matrix. The proliferation rate of studied cell lines was similar to 2D growth - mitochondrial HER2-enhanced proliferation was dependent on its kinase activity. When assessing migration through collagen, cells were first forced to form spheroids growing in non-adherent environment. Spheroids are a favourite 3D models – cells maintain close interconnection and form various layers mimicking structural and biochemical properties of solid tumours (Kapałczyńska et al., 2018). When formed, spheroids were embedded into collagen and migration of single cells from spheroids was observed. The information not only about the motility itself but also about the ability to overcome the ECM obstacle was obtained from this model. Mitochondrial HER2 brought an advantage in migration through collagen, but unexpectedly, the feature was not dependent on the kinase activity of HER2-MTS.

Growth without adherence in agarose brought even more serious discrepancy between 2D and 3D environment. Single cells seeded in agarose have to overcome loss of adherence

and need to escape from anoikis. In this assay, the constitutively enhanced kinase activity of HER2-MTS V659E presented a huge disadvantage, as MDA MTS V659E cells formed colonies only extremely poorly. It seems that consequence of HER2 mitochondrial localization is in contrast with its kinase activity, when the latter is presented in excess. Mitochondrial HER2 might help in non-adherent growth independent of its kinase activity, while constitutive kinase activity in MDA MTS V659E cells impairs proliferation in agarose. The most probably this discrepancy is driven by high oxidative stress in MDA MTS V659E cells. To confirm this hypothesis each cell line was transformed with mitochondrially targeted catalase and SOD2, which decreased formation of ROS in mitochondria. Several experiments are in process while I'm writing this thesis, but the results are not yet clear.

3D experiments are more demanding and have lower reproducibility (Kapałczyńska et al., 2018). However, my results are very clear and in close agreement with *in vivo* observation. The situation in a mouse model follows the data describing non-adherent growth *in vitro*. MDA MTS V659E cells injected subcutaneously formed the smallest tumours among all studied cell lines. My observations confirm the need for 3D culturing to be implemented into common practice.

Does it really mean that the kinase activity of mitochondrial HER2 sensitizing tumour cells to cell death lowers the cancer progression? This question is still to be answered. As already written above: More than 90 % of patient mortality is not due to primary tumour but metastases (Talmadge and Fidler, 2010). And MDA MTS V659E cells exhibit increased motility both in 2D and 3D environment. Even though the primary tumour originating from these cells did not proliferate rapidly, the cells could be still very potent to form metastases.

Elevated respiration and overall enhanced global bioenergetic activity driven by PGC1-α caused pro-metastatic phenotype of breast cancer cells (Andrzejewski et al., 2017). High mitochondrial activity of MDA MTS V659E cells might also promote pro-metastatic behaviour. Maintaining highly active both glycolysis and OXPHOS contributes to plasticity of cancer cells in metastatic cascade (Lehuédé et al., 2016). At this time, one more experiment is in progress. Each cell line transfected by luciferase allowing visualization of single cancer cell in mouse body is being injected into mammary fat pad. This experiment will bring two new aspects: Firstly, we will be able to visualize metastases formation among the mouse body,

and secondly, cells injected into mammary fat pad will appear in more familiar environment than in subcutaneous tissue potentially more able to attach to ECM and form a tumour.

To evaluate the impact of mitochondrial HER2 in breast cancer progression, quantification of the mitochondrial portion of HER2 in HER2^{high} breast cancer patient's derived samples would be required. Cell lines established in this study create a powerful experimental model but lack clinical relevance. HER2 localizes to the mitochondria due to its internal MTS, but our model of mitochondrial HER2 contains additional and more effective MTS derived from COX8. Moreover, the oncogenic potential of HER2 lies in its amplification in breast cancer, but presence of mutations is rare. Therefore, it can be expected that the effect of mitochondrial HER2 in clinics will be lesser than in model cell lines. On the other hand, it can be anticipated that lower amount of mitochondrial HER2 and its unaffected kinase activity will not impair cancer cell viability, as it does in MDA MTS V659E cells, and might still promote tumorigenesis. Further investigations could uncover the role of mitochondrial HER2 in levels present in HER2^{high} breast cancer. I would find convenient to track further treatment and long-term health condition of involved patients. Clinical studies denote many obstacles, though. Hopefully, we will be able to finish the project uncovering the clinical impact.

6 Summary

Even though HER2 has been studied extensively in past decades, its localization into mitochondria is usually neglected by the scientific community. As only little had been known about mitochondrial HER2, answering my opening questions has been challenging. As admitted in the discussion, not all the questions could be answered fully and convincingly. The initial simple hypothesis that the role of mitochondrial HER2 is dependent on its tyrosine kinase activity has proven more complicated, and it really seems that the right dozing is the key; too much is of it is detrimental. Rather, there seems to be a sweet spot which provides the maximal advantage. Even though I uncovered some of the answers in my thesis, the research continues and I'm looking forward to findings that will complete my study.

Here I would like to answer the questions I have set previously:

What is the function of mitochondrial pool of HER2 in breast cancer? Mitochondrial HER2 alters main bioenergetics pathways and it is independent on canonical AKT pathway. HER2-MTS promotes tumour cell proliferation and migration *in vitro* and primary tumour formation *in vivo*. Elevated level of ROS in this cell line tightly correlates with observed phenotype. However, it is unclear whether ROS production is a cause or a consequence of changes in cell metabolism.

Is the function of mitochondrial HER2 dependent on its tyrosine kinase activity? Several features caused by mitochondrial HER2 are dependent on its tyrosine kinase activity. Unexpectedly, kinase dead mutant exhibited elevated growth *in vivo* correlating with successful non-adherent growth and migration in collagen compared to other cell lines. The most probably, some other mechanism of mitochondrial HER2 action is also involved – potentially direct contact of mitochondrial HER2 with proteins of the respiratory chain.

Does tyrosine activity of mitochondrial HER2 sensitize cells to MitoTam agent? Yes, tyrosine kinase activity of mitochondrial HER2 clearly sensitizes breast cancer cells to MitoTam, the most probably due to elevated basal level of ROS.

7 Literature

Secondary citations are marked by asterisk.

Aceto, N., Bardia, A., Miyamoto, D.T., Donaldson, M.C., Wittner, B.S., Spencer, J.A., Yu, M., Pely, A., Engstrom, A., Zhu, H., *et al.* (2014). Circulating tumor cell clusters are oligoclonal precursors of breast cancer metastasis. Cell *158*, 1110-1122.

* Acin-Perez, R., and Enriquez, J.A. (2014). The function of the respiratory supercomplexes: the plasticity model. Biochimica et biophysica acta *1837*, 444-450.

Aguirre-Ghiso, J.A., and Sosa, M.S. (2018). Emerging Topics on Disseminated Cancer Cell Dormancy and the Paradigm of Metastasis. Annual Review of Cancer Biology *2*, 377-393.

Akiyama, T., Matsuda, S., Namba, Y., Saito, T., Toyoshima, K., and Yamamoto, T. (1991). The transforming potential of the c-erbB-2 protein is regulated by its autophosphorylation at the carboxyl-terminal domain. Molecular and Cellular Biology *11*, 833-842.

Andrzejewski, S., Klimcakova, E., Johnson, R.M., Tabaries, S., Annis, M.G., McGuirk, S., Northey, J.J., Chenard, V., Sriram, U., Papadopoli, D.J., *et al.* (2017). PGC-1alpha Promotes Breast Cancer Metastasis and Confers Bioenergetic Flexibility against Metabolic Drugs. Cell Metab *26*, 778-787.e775.

Antico Arciuch, V.G., Galli, S., Franco, M.C., Lam, P.Y., Cadenas, E., Carreras, M.C., and Poderoso, J.J. (2009). Akt1 intramitochondrial cycling is a crucial step in the redox modulation of cell cycle progression. PLoS One *4*, e7523.

Arena, G., Cissé, M.Y., Pyrdziak, S., Chatre, L., Riscal, R., Fuentes, M., Arnold, J.J., Kastner, M., Gayte, L., Bertrand-Gaday, C., *et al.* (2018). Mitochondrial MDM2 Regulates Respiratory Complex I Activity Independently of p53. Molecular Cell *69*, 594-609.e598.

Bajzikova, M., Kovarova, J., Coelho, A.R., Boukalova, S., Oh, S., Rohlenova, K., Svec, D., Hubackova, S., Endaya, B., Judasova, K., *et al.* (2019). Reactivation of Dihydroorotate Dehydrogenase-Driven Pyrimidine Biosynthesis Restores Tumor Growth of Respiration-Deficient Cancer Cells. Cell Metab *29*, 399-416.e310.

Barthel, A., Okino, S.T., Liao, J., Nakatani, K., Li, J., Whitlock, J.P., Jr., and Roth, R.A. (1999). Regulation of GLUT1 gene transcription by the serine/threonine kinase Akt1. J Biol Chem *274*, 20281-20286.

Biscardi, J.S., Belsches, A.P., and Parsons, S.J. (1998). Characterization of human epidermal growth factor receptor and c-Src interactions in human breast tumor cells. Molecular carcinogenesis *21*, 261-272.

Bray, F., Ferlay, J., Soerjomataram, I., Siegel, R.L., Torre, L.A., and Jemal, A. (2018). Global cancer statistics 2018: GLOBOCAN estimates of incidence and mortality worldwide for 36 cancers in 185 countries. CA: a cancer journal for clinicians *68*, 394-424.

Britsch, S., Li, L., Kirchhoff, S., Theuring, F., Brinkmann, V., Birchmeier, C., and Riethmacher, D. (1998). The ErbB2 and ErbB3 receptors and their ligand, neuregulin-1, are essential

for development of the sympathetic nervous system. Genes & development *12*, 1825-1836.

Calvo, S.E., Clauser, K.R., and Mootha, V.K. (2016). MitoCarta2.0: an updated inventory of mammalian mitochondrial proteins. Nucleic acids research *44*, D1251-1257.

Cavalli, L.R., Varella-Garcia, M., and Liang, B.C. (1997). Diminished tumorigenic phenotype after depletion of mitochondrial DNA. Cell growth & differentiation: the molecular biology journal of the American Association for Cancer Research *8*, 1189-1198.

Coussens, L., Yang-Feng, T.L., Liao, Y.C., Chen, E., Gray, A., McGrath, J., Seeburg, P.H., Libermann, T.A., Schlessinger, J., Francke, U., *et al.* (1985). Tyrosine kinase receptor with extensive homology to EGF receptor shares chromosomal location with neu oncogene. Science (New York, NY) *230*, 1132.

Croucher, D.R., Iconomou, M., Hastings, J.F., Kennedy, S.P., Han, J.Z.R., Shearer, R.F., McKenna, J., Wan, A., Lau, J., Aparicio, S., *et al.* (2016). Bimolecular complementation affinity purification (BiCAP) reveals dimer-specific protein interactions for ERBB2 dimers. Science Signaling *9*, ra69.

DeBerardinis, R.J., Mancuso, A., Daikhin, E., Nissim, I., Yudkoff, M., Wehrli, S., and Thompson, C.B. (2007). Beyond aerobic glycolysis: transformed cells can engage in glutamine metabolism that exceeds the requirement for protein and nucleotide synthesis. Proc Natl Acad Sci USA *104*, 19345-19350.

Demory, M.L., Boerner, J.L., Davidson, R., Faust, W., Miyake, T., Lee, I., Hüttemann, M., Douglas, R., Haddad, G., and Parsons, S.J. (2009). Epidermal growth factor receptor translocation to the mitochondria: regulation and effect. The Journal of biological chemistry *284*, 36592-36604.

Deprez, J., Vertommen, D., Alessi, D.R., Hue, L., and Rider, M.H. (1997). Phosphorylation and activation of heart 6-phosphofructo-2-kinase by protein kinase B and other protein kinases of the insulin signaling cascades. J Biol Chem *272*, 17269-17275.

Ding, Y., Liu, Z., Desai, S., Zhao, Y., Liu, H., Pannell, L.K., Yi, H., Wright, E.R., Owen, L.B., Dean-Colomb, W., *et al.* (2012). Receptor tyrosine kinase ErbB2 translocates into mitochondria and regulates cellular metabolism. Nature communications *3*, 1271.

Dušek L., M.J., Kubásek M., Koptíková J., Žaloudík J., Vyzula R. (2019). Epidemiologie zhoubných nádorů v České republice [online]. Masarykova univerzita, [2005], [cit. 2019-6-21]. Dostupný z WWW: http://www.svod.cz. Verze 7.0 [2007], ISSN 1802 – 8861.

Ferlay, J., Soerjomataram, I., Dikshit, R., Eser, S., Mathers, C., Rebelo, M., Parkin, D.M., Forman, D., and Bray, F. (2015). Cancer incidence and mortality worldwide: sources, methods and major patterns in GLOBOCAN 2012. International journal of cancer *136*, E359-386.

Gassmann, M., Casagranda, F., Orioli, D., Simon, H., Lai, C., Klein, R., and Lemke, G. (1995). Aberrant neural and cardiac development in mice lacking the ErbB4 neuregulin receptor. Nature *378*, 390-394.

Goldhirsch, A., Winer, E.P., Coates, A.S., Gelber, R.D., Piccart-Gebhart, M., Thürlimann, B., Senn, H.J., and Panel, m. (2013). Personalizing the treatment of women with early breast cancer: highlights of the St Gallen International Expert Consensus on the Primary Therapy of Early Breast Cancer 2013. Annals of oncology: official journal of the European Society for Medical Oncology *24*, 2206-2223.

Hackenbrock, C.R., Chazotte, B., and Gupte, S.S. (1986). The random collision model and a critical assessment of diffusion and collision in mitochondrial electron transport. Journal of bioenergetics and biomembranes *18*, 331-368.

Hamburger, A.W., and Salmon, S.E. (1977). Primary bioassay of human tumor stem cells. Science (New York, NY) *197*, 461-463.

* Hanahan, D., and Weinberg, R.A. (2000). The hallmarks of cancer. Cell *100*, 57-70.

* Hanahan, D., and Weinberg, Robert A. (2011). Hallmarks of Cancer: The Next Generation. Cell *144*, 646-674.

Howlader N., N.A.M., Krapcho M., Miller D., Bishop K., Kosary C.L., Yu M., Ruhl J., Tatalovich Z., Mariotto A., Lewis D.R., Chen H.S., Feuer E.J., Cronin K.A. (eds). (2017). SEER Cancer Statistics Review, 1975-2014, National Cancer Institute. Bethesda, MD, https://seer.cancer.gov/csr/1975_2014/, based on November 2016 SEER data submission, posted to the SEER web site, April 2017.

* Hsu, J.L., and Hung, M.C. (2016). The role of HER2, EGFR, and other receptor tyrosine kinases in breast cancer. Cancer metastasis reviews *35*, 575-588.

* Hynes, N.E., and Lane, H.A. (2005). ERBB receptors and cancer: the complexity of targeted inhibitors. Nature reviews Cancer *5*, 341-354.

Chance, B., and Williams, G.R. (1955). A method for the localization of sites for oxidative phosphorylation. Nature *176*, 250-254.

Iskandar, K., Rezlan, M., Yadav, S.K., Foo, C.H., Sethi, G., Qiang, Y., Bellot, G.L., and Pervaiz, S. (2016). Synthetic Lethality of a Novel Small Molecule Against Mutant KRAS-Expressing Cancer Cells Involves AKT-Dependent ROS Production. Antioxidants & redox signaling *24*, 781-794.

* Jiang, W.G., Sanders, A.J., Katoh, M., Ungefroren, H., Gieseler, F., Prince, M., Thompson, S.K., Zollo, M., Spano, D., Dhawan, P., *et al.* (2015). Tissue invasion and metastasis: Molecular, biological and clinical perspectives. Seminars in Cancer Biology *35*, S244-S275.

* Kapałczyńska, M., Kolenda, T., Przybyła, W., Zajączkowska, M., Teresiak, A., Filas, V., Ibbs, M., Bliźniak, R., Łuczewski, Ł., and Lamperska, K. (2018). 2D and 3D cell cultures - a comparison of different types of cancer cell cultures. Arch Med Sci *14*, 910-919.

Kaplan, R.N., Rafii, S., and Lyden, D. (2006). Preparing the "soil": the premetastatic niche. Cancer research *66*, 11089-11093.

Katt, M.E., Placone, A.L., Wong, A.D., Xu, Z.S., and Searson, P.C. (2016). In Vitro Tumor Models: Advantages, Disadvantages, Variables, and Selecting the Right Platform. Frontiers in bioengineering and biotechnology *4*, 12.

Khan, A.U.H., Rathore, M.G., Allende-Vega, N., Vo, D.-N., Belkhala, S., Orecchioni, S., Talarico, G., Bertolini, F., Cartron, G., Lecellier, C.-H., *et al.* (2016). Human Leukemic Cells performing Oxidative Phosphorylation (OXPHOS) Generate an Antioxidant Response Independently of Reactive Oxygen species (ROS) Production. EBioMedicine *3*, 43-53.

Kilian, K.A., Bugarija, B., Lahn, B.T., and Mrksich, M. (2010). Geometric cues for directing the differentiation of mesenchymal stem cells. Proc Natl Acad Sci USA *107*, 4872-4877.

King, C.R., Kraus, M.H., and Aaronson, S.A. (1985). Amplification of a novel v-erbB-related gene in a human mammary carcinoma. Science (New York, NY) *229*, 974-976.

Kluckova, K., Dong, L.F., Bajzikova, M., Rohlena, J., and Neuzil, J. (2015). Evaluation of respiration of mitochondria in cancer cells exposed to mitochondria-targeted agents. Methods in molecular biology (Clifton, NJ) *1265*, 181-194.

Kurien, B.T., and Scofield, R.H. (2006). Western blotting. Methods (San Diego, Calif) *38*, 283-293.

Laemmli, U.K. (1970). Cleavage of Structural Proteins during the Assembly of the Head of Bacteriophage T4. Nature *227*, 680-685.

Lapuente-Brun, E., Moreno-Loshuertos, R., Acín-Pérez, R., Latorre-Pellicer, A., Colás, C., Balsa, E., Perales-Clemente, E., Quirós, P.M., Calvo, E., Rodríguez-Hernández, M.A., *et al.* (2013). Supercomplex Assembly Determines Electron Flux in the Mitochondrial Electron Transport Chain. Science (New York, NY) *340*, 1567-1570.

Lee, K.F., Simon, H., Chen, H., Bates, B., Hung, M.C., and Hauser, C. (1995). Requirement for neuregulin receptor erbB2 in neural and cardiac development. Nature *378*, 394-398.

* Lehuédé, C., Dupuy, F., Rabinovitch, R., Jones, R.G., and Siegel, P.M. (2016). Metabolic Plasticity as a Determinant of Tumor Growth and Metastasis. Cancer research *76*, 5201-5208.

Lemmens, K., Doggen, K., and De Keulenaer, G.W. (2011). Activation of the neuregulin/ErbB system during physiological ventricular remodeling in pregnancy. American journal of physiology Heart and circulatory physiology *300*, H931-942.

Leslie, N.R., Bennett, D., Lindsay, Y.E., Stewart, H., Gray, A., and Downes, C.P. (2003). Redox regulation of PI 3-kinase signalling via inactivation of PTEN. The EMBO Journal *22*, 5501-5510.

* Liemburg-Apers, D.C., Willems, P.H.G.M., Koopman, W.J.H., and Grefte, S. (2015). Interactions between mitochondrial reactive oxygen species and cellular glucose metabolism. Arch Toxicol *89*, 1209-1226.

Liu, X., Hwang, H., Cao, L., Buckland, M., Cunningham, A., Chen, J., Chien, K.R., Graham, R.M., and Zhou, M. (1998). Domain-specific gene disruption reveals critical regulation

of neuregulin signaling by its cytoplasmic tail. Proceedings of the National Academy of Sciences *95*, 13024.

* Loibl, S., and Gianni, L. (2017). HER2-positive breast cancer. Lancet (London, England) *389*, 2415-2429.

Lopez-Fabuel, I., Le Douce, J., Logan, A., James, A.M., Bonvento, G., Murphy, M.P., Almeida, A., and Bolaños, J.P. (2016). Complex I assembly into supercomplexes determines differential mitochondrial ROS production in neurons and astrocytes. Proceedings of the National Academy of Sciences *113*, 13063-13068.

* Mathupala, S.P., Ko, Y.H., and Pedersen, P.L. (2006). Hexokinase II: cancer's double-edged sword acting as both facilitator and gatekeeper of malignancy when bound to mitochondria. Oncogene *25*, 4777-4786.

Maurer, U., Charvet, C., Wagman, A.S., Dejardin, E., and Green, D.R. (2006). Glycogen synthase kinase-3 regulates mitochondrial outer membrane permeabilization and apoptosis by destabilization of MCL-1. Mol Cell *21*, 749-760.

Mehta, F., Theunissen, R., and Post, M.J. (2019). Adipogenesis from Bovine Precursors. Methods in molecular biology (Clifton, NJ) *1889*, 111-125.

Meyer, D., and Birchmeier, C. (1995). Multiple essential functions of neuregulin in development. Nature *378*, 386-390.

Mihara, M., Erster, S., Zaika, A., Petrenko, O., Chittenden, T., Pancoska, P., and Moll, U.M. (2003). p53 Has a Direct Apoptogenic Role at the Mitochondria. Molecular Cell *11*, 577-590.

* Mishra, R., Patel, H., Alanazi, S., Yuan, L., and Garrett, J.T. (2018). HER3 signaling and targeted therapy in cancer. Oncology reviews *12*, 355-355.

Mitchell, P. (1961). Coupling of phosphorylation to electron and hydrogen transfer by a chemi-osmotic type of mechanism. Nature *191*, 144-148.

Mitsumoto, Y., and Klip, A. (1992). Development regulation of the subcellular distribution and glycosylation of GLUT1 and GLUT4 glucose transporters during myogenesis of L6 muscle cells. J Biol Chem *267*, 4957-4962.

* Moloney, J.N., and Cotter, T.G. (2018). ROS signalling in the biology of cancer. Seminars in Cell & Developmental Biology *80*, 50-64.

Morais, R., Zinkewich-Peotti, K., Parent, M., Wang, H., Babai, F., and Zollinger, M. (1994). Tumor-forming ability in athymic nude mice of human cell lines devoid of mitochondrial DNA. Cancer research *54*, 3889-3896.

Mori, S., Akiyama, T., Yamada, Y., Morishita, Y., Sugawara, I., Toyoshima, K., and Yamamoto, T. (1989). C-erbB-2 gene product, a membrane protein commonly expressed on human fetal epithelial cells. Laboratory investigation; a journal of technical methods and pathology *61*, 93-97.

Nagata, Y., Lan, K.H., Zhou, X., Tan, M., Esteva, F.J., Sahin, A.A., Klos, K.S., Li, P., Monia, B.P., Nguyen, N.T., *et al.* (2004). PTEN activation contributes to tumor inhibition by

trastuzumab, and loss of PTEN predicts trastuzumab resistance in patients. Cancer cell *6*, 117-127.

Naresh, A., Thor, A.D., Edgerton, S.M., Torkko, K.C., Kumar, R., and Jones, F.E. (2008). The HER4/4ICD estrogen receptor coactivator and BH3-only protein is an effector of tamoxifen-induced apoptosis. Cancer research *68*, 6387-6395.

* Nelson, C.M., and Bissell, M.J. (2006). Of extracellular matrix, scaffolds, and signaling: tissue architecture regulates development, homeostasis, and cancer. Annu Rev Cell Dev Biol *22*, 287-309.

* Odiete, O., Hill, M.F., and Sawyer, D.B. (2012). Neuregulin in cardiovascular development and disease. Circulation research *111*, 1376-1385.

* Osaki, M., Oshimura, M., and Ito, H. (2004). PI3K-Akt pathway: Its functions and alterations in human cancer. Apoptosis *9*, 667-676.

Paget, S. (1889). The distribution of secondary growths in cancer of the breast. The Lancet *133*, 571-573.

Pastorino, J.G., Hoek, J.B., and Shulga, N. (2005). Activation of glycogen synthase kinase 3beta disrupts the binding of hexokinase II to mitochondria by phosphorylating voltage-dependent anion channel and potentiates chemotherapy-induced cytotoxicity. Cancer research *65*, 10545-10554.

Pedram, A., Razandi, M., Wallace, D.C., and Levin, E.R. (2006). Functional Estrogen Receptors in the Mitochondria of Breast Cancer Cells. Molecular Biology of the Cell *17*, 2125-2137.

Pesta, D., and Gnaiger, E. (2012). High-resolution respirometry: OXPHOS protocols for human cells and permeabilized fibers from small biopsies of human muscle. Methods in molecular biology (Clifton, NJ) *810*, 25-58.

Ram, T.G., and Ethier, S.P. (1996). Phosphatidylinositol 3-kinase recruitment by p185erbB-2 and erbB-3 is potently induced by neu differentiation factor/heregulin during mitogenesis and is constitutively elevated in growth factor-independent breast carcinoma cells with c-erbB-2 gene amplification. Cell growth & differentiation: the molecular biology journal of the American Association for Cancer Research *7*, 551-561.

Ravid-Hermesh, O., Zurgil, N., Shafran, Y., Afrimzon, E., Sobolev, M., Hakuk, Y., Bar-On Eizig, Z., and Deutsch, M. (2018). Analysis of Cancer Cell Invasion and Anti-metastatic Drug Screening Using Hydrogel Micro-chamber Array (HMCA)-based Plates. Journal of visualized experiments: JoVE.

Remels, A.H., Langen, R.C., Schrauwen, P., Schaart, G., Schols, A.M., and Gosker, H.R. (2010). Regulation of mitochondrial biogenesis during myogenesis. Molecular and cellular endocrinology *315*, 113-120.

* Rivera, E., and Gomez, H. (2010). Chemotherapy resistance in metastatic breast cancer: the evolving role of ixabepilone. Breast Cancer Research *12*, S2.

Rohlenova, K., Sachaphibulkij, K., Stursa, J., Bezawork-Geleta, A., Blecha, J., Endaya, B., Werner, L., Cerny, J., Zobalova, R., Goodwin, J., *et al.* (2017). Selective Disruption of

Respiratory Supercomplexes as a New Strategy to Suppress Her2(high) Breast Cancer. Antioxidants & redox signaling *26*, 84-103.

Rohrbach, S., Niemann, B., Silber, R.E., and Holtz, J. (2005). Neuregulin receptors erbB2 and erbB4 in failing human myocardium -- depressed expression and attenuated activation. Basic research in cardiology *100*, 240-249.

Ruiz-Saenz, A., Dreyer, C., Campbell, M.R., Steri, V., Gulizia, N., and Moasser, M.M. (2018). HER2 Amplification in Tumors Activates PI3K/Akt Signaling Independent of HER3. Cancer research *78*, 3645-3658.

* Saraste, M. (1999). Oxidative Phosphorylation at the fin de siècle. Science (New York, NY) *283*, 1488-1493.

Schägger, H., and Pfeiffer, K. (2000). Supercomplexes in the respiratory chains of yeast and mammalian mitochondria. The EMBO Journal *19*, 1777-1783.

Schägger, H., and von Jagow, G. (1991). Blue native electrophoresis for isolation of membrane protein complexes in enzymatically active form. Analytical biochemistry *199*, 223-231.

Schillaci, R., Guzman, P., Cayrol, F., Beguelin, W., Diaz Flaque, M.C., Proietti, C.J., Pineda, V., Palazzi, J., Frahm, I., Charreau, E.H., *et al.* (2012). Clinical relevance of ErbB-2/HER2 nuclear expression in breast cancer. BMC cancer *12*, 74.

* Schramm, A., De Gregorio, N., Widschwendter, P., Fink, V., and Huober, J. (2015). Targeted Therapies in HER2-Positive Breast Cancer - a Systematic Review. Breast Care (Basel) *10*, 173-178.

Schulze, W.X., Deng, L., and Mann, M. (2005). Phosphotyrosine interactome of the ErbB-receptor kinase family. Molecular systems biology *1*, 2005.0008-2005.0008.

Slamon, D.J., Clark, G.M., Wong, S.G., Levin, W.J., Ullrich, A., and McGuire, W.L. (1987). Human breast cancer: correlation of relapse and survival with amplification of the HER-2/neu oncogene. Science (New York, NY) *235*, 177-182.

* Slater, E.C. (2003). Keilin, cytochrome, and the respiratory chain. J Biol Chem *278*, 16455-16461.

Sonveaux, P., Végran, F., Schroeder, T., Wergin, M.C., Verrax, J., Rabbani, Z.N., De Saedeleer, C.J., Kennedy, K.M., Diepart, C., Jordan, B.F., *et al.* (2008). Targeting lactate-fueled respiration selectively kills hypoxic tumor cells in mice. J Clin Invest *118*, 3930-3942.

* Talmadge, J.E., and Fidler, I.J. (2010). AACR Centennial Series: The Biology of Cancer Metastasis: Historical Perspective. Cancer research *70*, 5649.

Tan, An S., Baty, James W., Dong, L.-F., Bezawork-Geleta, A., Endaya, B., Goodwin, J., Bajzikova, M., Kovarova, J., Peterka, M., Yan, B., *et al.* (2015). Mitochondrial Genome Acquisition Restores Respiratory Function and Tumorigenic Potential of Cancer Cells without Mitochondrial DNA. Cell Metabolism *21*, 81-94.

Tzahar, E., Waterman, H., Chen, X., Levkowitz, G., Karunagaran, D., Lavi, S., Ratzkin, B.J., and Yarden, Y. (1996). A hierarchical network of interreceptor interactions determines

signal transduction by Neu differentiation factor/neuregulin and epidermal growth factor. Molecular and cellular biology *16*, 5276-5287.

* Vander Heiden, M.G., Cantley, L.C., and Thompson, C.B. (2009). Understanding the Warburg effect: the metabolic requirements of cell proliferation. Science (New York, NY) *324*, 1029-1033.

Venneti, S., Dunphy, M.P., Zhang, H., Pitter, K.L., Zanzonico, P., Campos, C., Carlin, S.D., La Rocca, G., Lyashchenko, S., Ploessl, K., *et al.* (2015). Glutamine-based PET imaging facilitates enhanced metabolic evaluation of gliomas in vivo. Science Translational Medicine *7*, 274ra217-274ra217.

Vogel, C.L., Cobleigh, M.A., Tripathy, D., Gutheil, J.C., Harris, L.N., Fehrenbacher, L., Slamon, D.J., Murphy, M., Novotny, W.F., Burchmore, M., *et al.* (2002). Efficacy and safety of trastuzumab as a single agent in first-line treatment of HER2-overexpressing metastatic breast cancer. Journal of clinical oncology : official journal of the American Society of Clinical Oncology *20*, 719-726.

von der Mark, K., Gauss, V., von der Mark, H., and Muller, P. (1977). Relationship between cell shape and type of collagen synthesised as chondrocytes lose their cartilage phenotype in culture. Nature *267*, 531-532.

Vondrusova, M., Bezawork-Geleta, A., Sachaphibulkij, K., Truksa, J., and Neuzil, J. (2015). The effect of mitochondrially targeted anticancer agents on mitochondrial (super)complexes. Methods in molecular biology (Clifton, NJ) *1265*, 195-208.

Wang, S.C., Lien, H.C., Xia, W., Chen, I.F., Lo, H.W., Wang, Z., Ali-Seyed, M., Lee, D.F., Bartholomeusz, G., Ou-Yang, F., *et al.* (2004). Binding at and transactivation of the COX-2 promoter by nuclear tyrosine kinase receptor ErbB-2. Cancer cell *6*, 251-261.

Warburg, O. (1924). Über den Stoffwechsel der Carcinomzelle. Naturwissenschaften *12*, 1131-1137.

Warburg, O. (1956). On the origin of cancer cells. Science (New York, NY) *123*, 309-314.

Waterman, H., and Yarden, Y. (2001). Molecular mechanisms underlying endocytosis and sorting of ErbB receptor tyrosine kinases. FEBS letters *490*, 142-152.

* Welch, D.R., and Hurst, D.R. (2019). Defining the Hallmarks of Metastasis. Cancer research.

Wittig, I., Braun, H.P., and Schagger, H. (2006). Blue native PAGE. Nature protocols *1*, 418-428.

* Yarden, Y., and Sliwkowski, M.X. (2001). Untangling the ErbB signalling network. Nat Rev Mol Cell Biol *2*, 127-137.